CONFIDENTIAL

NACA RM L52K12

NACA

RESEARCH MEMORANDUM

LONGITUDINAL-CONTROL EFFECTIVENESS AND DOWNWASH CHARACTERISTICS AT TRANSONIC SPEEDS OF A $\frac{1}{30}$-SCALE SEMISPAN MODEL OF THE BELL X-5 AIRPLANE AS DETERMINED BY THE NACA WING-FLOW METHOD

By Norman S. Silsby and Garland J. Morris

Langley Aeronautical Laboratory
Langley Field, Va.

NATIONAL ADVISORY COMMITTEE FOR AERONAUTICS

WASHINGTON

January 12, 1953

CONFIDENTIAL

NATIONAL ADVISORY COMMITTEE FOR AERONAUTICS

RESEARCH MEMORANDUM

LONGITUDINAL-CONTROL EFFECTIVENESS AND DOWNWASH CHARACTERISTICS AT TRANSONIC SPEEDS OF A $\frac{1}{30}$ - SCALE SEMISPAN MODEL OF THE BELL X-5 AIRPLANE AS DETERMINED BY THE NACA WING-FLOW METHOD

By Norman S. Silsby and Garland J. Morris

SUMMARY

An investigation has been made at transonic speeds by the NACA wing-flow method to determine the longitudinal-control effectiveness and downwash characteristics of a $\frac{1}{30}$ - scale semispan model of the Bell X-5 airplane with the wing sweptback 60°, 40°, and 20°. Lift, drag, and pitching moment were obtained for various angles of attack for several horizontal-tail settings and with tail off for each angle of sweep tested. The Reynolds number was about 1.0×10^6.

There was an instability for both tail-on and tail-off configurations above an angle of attack of about 8.5° for the model with the 60° sweptback wing over a Mach number range from 0.83 to 1.00, and above about 5° angle of attack for the model with the 40° sweptback wing at Mach numbers from 0.7 to 0.94. The effectiveness of the stabilizer in producing pitching-moment variations appeared to be linear over the range of deflections tested and was affected relatively little by Mach number, angle of attack (up to 8°), or sweep angle. On the basis of the results, to trim the full-scale airplane in level flight at Mach numbers from 0.75 to 1.05 required a gradual change in stabilizer angle covering a range of 4° at 40,000 feet altitude and about 3° at 20,000 feet for the airplane with the 60° wing, and 1° or less change of stabilizer angle for the airplane with wings of 40° or 20° sweep at either altitude; the variations with Mach number of stabilizer angle required for trim was stable over the range tested for the three sweep angles at both altitudes, except for the 20° configuration which showed a slightly unstable variation above a Mach number of about 0.9 at both altitudes. For all three swept wings tested, the values of the rate of change of downwash angle with angle of attack increased gradually with increasing Mach number so that maximum values were reached at progressively higher Mach numbers (less than 1.00) in the order of increasing sweepback, after which there was a decrease with further increase in Mach number.

INTRODUCTION

As part of a program to determine the aerodynamic characteristics of the Bell X-5 airplane incorporating a wing whose angle of sweep can be varied in flight, an investigation has been made at transonic speeds by the NACA wing-flow method on a $\frac{1}{30}$-scale semispan model. The semispan model tested differed from the full-scale airplane in that the model had trailing-edge wing fillets at all sweep angles except 60°. The wing pivot locations, mean aerodynamic chords, and location of the mean aerodynamic chords of the model did not correspond exactly with those of the full-scale airplane. Results of tests at a Mach number of 1.24 have been reported in references 1 to 5. The first report on results of tests at transonic speeds (ref. 6) presents the effect of sweepback on the longitudinal force characteristics for a tail incidence of -2°. The results presented herein consist of measurements of lift, drag, and pitching moment obtained in tests of the model over a range of angle of attack with tail incidences of 0°, -4°, and -6° with the wing swept back 60°, and a tail incidence of -6° with the wing swept back 40° and 20°. Measurements were also made for each sweepback angle with the tail off. These data together with those of reference 6 are used to determine the stabilizer effectiveness and downwash characteristics of the model. The effective Mach number at the wing of the model for the tests covered a range from about 0.7 to 1.05 and the Reynolds number was of the order of 1.0×10^6.

SYMBOLS

$b/2$ model wing span, in.

c local wing chord parallel to plane of symmetry, in.

$\bar{c}$ mean aerodynamic chord of wing based on the relationship

$$\frac{\int_0^{b/2} c^2 dy}{\int_0^{b/2} c\, dy}, \text{ in.}$$

$\bar{c}_t$ mean aerodynamic chord of tail, in.

C_D drag coefficient, $\frac{D}{qS}$

$C_{D_{C_L=0}}$ drag coefficient at zero lift

C_L lift coefficient, $\frac{L}{qS}$

C_m pitching-moment coefficient about center line of balance (center-of-gravity location of full-scale airplane), $\frac{M}{qS\bar{c}}$

$\frac{dC_L}{d\alpha}$ rate of change of lift coefficient with angle of attack

$\frac{\partial C_m}{\partial C_L}$ rate of change of pitching-moment coefficient with lift coefficient

D drag, lb

$\frac{\partial C_m}{\partial i_t}$ effectiveness of horizontal tail, per deg

$\frac{d\epsilon}{d\alpha}$ effective rate of change of downwash angle with angle of attack

H_p pressure altitude, ft

i_t incidence of horizontal tail (referred to wing-chord plane), deg

L lift, lb

M pitching moment, in-lb

M_L local Mach number at wing surface of F-51D airplane

M_t effective Mach number for tail of model

M_w effective Mach number for wing of model

q effective dynamic pressure for wing of model, lb/sq ft

R_w Reynolds number for wing of model based on mean aerodynamic chord $\bar{c}$

R_t Reynolds number based on $\bar{c}_t$

S wing area, semispan model (position of wing within fuselage is considered to be formed by perpendiculars from wing-fuselage intersections to plane of symmetry), $\int_0^{b/2} c\,dy$, sq ft

y spanwise coordinate, in.

α angle of attack (referred to wing-chord plane), deg

ϵ effective downwash angle at tail of model, deg

Λ sweepback angle referred to 25-percent chord line of 50° sweptback wing

A prime indicates coefficients based on dimensions of configuration with 60° sweptback wing.

APPARATUS AND TESTS

The tests were made by the NACA wing-flow method in which the model is mounted in a region of high-speed flow over the wing of an F-51D airplane.

The configurations tested and reported herein consisted of the $\frac{1}{30}$-scale semispan model of the Bell X-5 airplane equipped successively with a 60° sweptback wing for tail incidences of 0°, -4°, and -6°, and with wings of 40° and 20° sweepback angles for a tail incidence of -6°. The model was also tested with tail off for each angle of sweep of the wing.

Geometric characteristics of the model pertinent to the present tests are given in table I and in figure 1. Photographs of various configurations of the model are shown in figures 2 and 3. Further details of the model construction may be found in references 1 to 6. The model was originally designed and constructed so that the pitching moment would be measured about the gross weight center-of-gravity location for the full-scale airplane. This center-of-gravity location corresponded to the 25 percent mean aerodynamic chord of the wing in each sweep position. However, some changes in the design of the full-scale airplane, specifically, a reduction in wing span and the addition of a trailing-edge fillet to the wings in all sweep positions except 60°, were incorporated in the semispan model before its construction was completed; these changes altered the mean aerodynamic chords and their locations so that the 26 percent mean aerodynamic chord of the 60° wing

and the 35 percent mean aerodynamic chord of the 40° and 20° wings correspond to the center-of-gravity position about which the pitching moments were taken. Still other changes in the airplane not incorporated in the semispan model of the present tests have altered both the trailing-edge fillets and the longitudinal location of the wings with respect to the fuselage, that is, the translational locations of the wing pivot point for the various sweep angles of the model do not correspond with those of the full-scale Bell X-5 airplane. Also, the mean aerodynamic chords and their relations to the pivot points are different because of the trailing-edge fillets on the model.

The mounting of the model and method of testing were similar to that described in reference 6. Because the model and balance were arranged to oscillate as a unit, forces were measured normal and parallel to the model fuselage reference line at all angles of attack. Continuous measurements were made of angle of attack, normal force, chord force and pitching moment as the model was oscillated at a rate of about 20 degrees per second through an angle-of-attack range of about -4° to 12°. A typical chordwise Mach number distribution in the test region on the airplane wing as determined from static-pressure measurements at the wing surface with the model removed is indicated in figure 4. The average vertical Mach number gradient, determined from static-pressure measurements made with a static-pressure tube located at various distances up to 6 inches above the surface of the test section, was found to be about -0.006 per inch. The effective dynamic pressure for the model wing q, the effective Mach number for the model wing M_w, and the effective Mach number for the model tail M_t were obtained from an integration of the Mach number distribution over the area covered by the wing and tail of the model. A more complete discussion of the method of determining the effective Mach number and dynamic pressure for the model may be found in reference 7. For the present tests, the Mach number for the wing of the model covered a range from about 0.7 to 1.05. The average relation between Reynolds number of the 60° sweptback wing R_w' and the Reynolds number of the tail R_t with the Mach number at the wing M_w is shown in figure 5. The Reynolds number for the wings other than the 60° sweptback wing can be found by multiplying the values of R_w' in figure 5 by the ratio of $\bar{c}$ of the wing desired to $\bar{c}$ of the 60° wing.

REDUCTION OF DATA

Sample data are shown in figure 6 for one oscillation through the angle-of-attack range. The Mach number M_w varied from 0.860 to 0.851 during the cycle. The curves faired through these points are used to give results for a Mach number of 0.856. Similarly, data for several

cycles were reduced for each configuration and cross plotted to show variations of the characteristics with Mach number at constant lift coefficients.

Lift, drag, and pitching-moment coefficients are based on the wing area extended to the fuselage center line as shown in figure 1. In the basic data presented in figures 7 to 9 the coefficients are based on respective wing dimensions; in all subsequent figures the coefficients are based on the dimensions of the 60° wing in order to indicate the characteristics of the model as for a variable sweep airplane.

All pitching-moment results are referred to the fuselage station on the model corresponding to the gross weight center of gravity of the full-scale airplane, such station corresponding to the 26 percent mean aerodynamic chord for the 60° wing, and the 35 percent mean aerodynamic chord for the 40° and 20° wings.

The values of $d\epsilon/d\alpha$ against Mach number for the model with the 60°, 40°, and 20° sweptback wings were obtained from the results given in figures 10 and 11 and from plots similar to these at various other Mach numbers within the range tested. The assumption was made that the downwash angle was equal to the sum of the tail incidence and the angle of attack at which the pitching moment for that particular tail incidence was equal to the pitching moment with tail off. Thus, curves of ϵ against α were determined for various Mach numbers and the slopes $d\epsilon/d\alpha$ were obtained. For the 40° and 20° sweptback wings, curves of ϵ against α were determined in a similar manner. However, in view of the limited data (only two tail incidences for these sweep angles) an average slope of $\partial C_m/\partial i_t$ of -0.0186 was used to draw the curves through the two data points for each α and cross plots at various intermediate tail incidences were made to establish curves of ϵ against α.

DISCUSSION OF RESULTS

The results are presented in figures 7 to 17. The quantities and configurations, and the figures in which they appear are presented in table II.

Lift, drag, and pitching moment.- The variation of lift coefficient with angle of attack and the variation of pitching-moment coefficient and drag coefficient with lift coefficient (figs. 10 to 12) for the model with various tail incidences indicate results similar to those for a tail incidence of -2° reported in reference 6 over a Mach number range from about 0.75 to 1.05. Further discussion of these characteristics will therefore not be given herein except in regard to longitudinal stability,

particularly at lift coefficients above 0.4, which was not discussed in the tests of reference 6.

Longitudinal stability.- A comparison of the variation of $\partial C_m'/\partial C_L'$ with Mach number at $C_L' = 0$ for the model equipped with the three sweptback wings for the various tail conditions (fig. 13(a)) indicates that the static margin (the difference between the neutral point and the center of gravity at 26 percent mean aerodynamic chord of the 60° sweptback wing) increases from 6 to 12 percent mean aerodynamic chord depending on the tail incidence and sweep angle with increase in Mach number from 0.7 to 1.05. At a lift coefficient of 0.4 the static margin increases with Mach number from about 11 to 21 percent mean aerodynamic chord of the 60° sweptback wing, a somewhat larger shift on the average than at $C_L' = 0$, at least for the tail-on conditions (fig. 13(b)). The static margin was substantially greater for the 60° wing at $C_L' = 0.4$ than that for both the 40° and 20° wings. An instability with increasing angle of attack for both tail-on and tail-off configurations occurs at angles of attack above about 8.5° for the configurations with the 60° sweptback wing over a Mach number range from 0.83 to 1.00 and above about 5° angle of attack for the model with the 40° sweptback wing from a Mach number of 0.7 (the lowest tested) up to about 0.94 (see fig. 14). The model with the 60° sweptback wing (tail on) again became stable above about 10.2° angle of attack up to the maximum α for the tests in a Mach number range from about 0.94 to 0.97. A slight tendency toward instability is indicated for the configuration with the 20° sweptback wing and $i_t = -2°$ at an angle of attack of about 9° for Mach numbers from 0.8 to 0.84.

Longitudinal-control effectiveness.- The slope of the variation of pitching-moment coefficient with tail incidence $\partial C_m'/\partial i_t$, which is regarded as the tail effectiveness parameter (fig. 16), is in the range from -0.017 to -0.020 for the Mach numbers tested for angles of attack up to 8° for the model with the 60° sweptback wing. The tail effectiveness parameter $\partial C_m'/\partial i_t$ was not definitely established for the 40° and 20° swept-wing configurations due to a limited number of test points, but the dashed lines of figure 15, representing an approximate fairing of C_m' against i_t for the 40° and 20° configurations, indicate essentially the same range of values of $\partial C_m'/\partial i_t$ as for the 60° wing for the conditions covered. Thus, for all configurations of the model tested and for angles of attack up to 8°, the effectiveness of the stabilizer in changing the pitching moment appears to be relatively constant over the Mach number range covered (0.75 to 1.05). The value of $\partial C_m'/\partial i_t$ obtained for similar configurations at a Mach number of 1.24 (ref. 3) was about -0.016 for all configurations, indicating only a slight reduction in tail effectiveness at low supersonic speeds over that at subsonic speeds. The values of $\partial C_m'/\partial i_t$ obtained in these tests and in those

of reference 3 may be slightly high because of the higher Mach number at the tail of the model due to the chordwise gradient (see fig. 4).

To trim the full-scale airplane in level flight at Mach numbers from 0.75 to 1.05 by assuming a wing loading of 50 pounds per square foot and a common center-of-gravity location (26 percent mean aerodynamic chord for the 60° sweptback wing, 35 percent mean aerodynamic chord for the 40° and 20° sweptback wings) requires a gradual change in stabilizer angle covering a range of 4° at 40,000 feet altitude and about 3° at 20,000 feet for the airplane with the 60° wing, and 1° or less change of stabilizer angle for the airplane with wings of 40° or 20° sweep at either altitude (see fig. 17). The relatively large trim change indicated for the 60° wing is principally due to the high static margin for the model with the 60° wing, and is not directly due to compressibility effects. Such high static margin would not be expected to be present in the full-scale airplane which employs a greater forward translation of the wing with increasing sweepback angle. The variation of stabilizer angle required for trim with Mach number is stable over the range tested for both the 60° and 40° configurations for the center-of-gravity location noted above; for the airplane with the wing sweptback 20° the variation with Mach number of stabilizer angle for trim was stable up to about $M = 0.90$ and slightly unstable with further increase in Mach number to 1.025, the maximum for the tests.

Downwash characteristics.- The absolute values of the effective downwash angles given in figure 18 are subject to some uncertainty for the following three reasons: (1) pitching moment due to drag of the tail was neglected, (2) the C_L at the tail may not be 0 at $\alpha_t = 0$ due to flow around the fuselage, and (3) unpublished results have indicated that there is a variation of about 1° in the direction of flow over the F-51D wing between the positions occupied by the wing and the tail of the X-5 semispan model. However, the variation of downwash angle with angle of attack and with lift coefficient determined by the method employed should not be affected by these contingencies. The values of $d\epsilon/d\alpha$ increase gradually with increasing high subsonic Mach numbers and reach a maximum value of 0.78 at $M_W = 0.9$ for the model with the 40° sweptback wing, 0.72 at $M_W = 0.85$ for the 20° configuration, and 0.54 at $M_W = 0.93$ for the 60° configuration; after these peaks there is a decrease with further increase in Mach number. The peak value of $d\epsilon/d\alpha$ occurs progressively at higher Mach numbers as the sweep angle increases from 20° to 60°. At any Mach number the value of $d\epsilon/d\alpha$, in general, increases with decreasing sweepback angle except in a range of Mach numbers from about 0.86 to 0.94 where the values of $d\epsilon/d\alpha$ are greater for the 40° configuration than for the model with the 20° sweptback wing. The value of $d\epsilon/d\alpha$ (0.40) for the 60° configuration in the Mach number range from 1.00 to 1.05 is only slightly greater than the value of 0.38 (also shown in fig. 18) obtained for the same configuration at a Mach number of 1.24 in the tests reported in reference 3.

CONCLUSIONS

The results of NACA wing-flow tests at transonic speeds to determine the longitudinal-control effectiveness and downwash characteristics of a $\frac{1}{30}$-scale semispan model of the Bell X-5 airplane may be summarized as follows:

(1) An instability with increasing angle of attack for both tail-on and tail-off configurations was indicated at angles of attack starting at about 8.5° for the model with the 60° sweptback wing over a Mach number range from 0.83 to 1.00, and above about 5° angle of attack for the model with the 40° sweptback wing at Mach numbers from 0.7 to 0.94.

(2) The effectiveness of the stabilizer in producing pitching-moment variations appeared to be linear over the range of deflections tested and was affected relatively little by Mach number, angle of attack, or sweep angle; the values of the stabilizer effectiveness parameter were in the range from -0.017 to -0.020 for all conditions covered.

(3) On the basis of the results, to trim the full-scale airplane in level flight at Mach numbers from 0.75 to 1.05 required a gradual decrease in stabilizer angle covering a range of 4° at 40,000 feet altitude and about 3° at 20,000 feet for the airplane with the 60° wing, and 1° or less change of stabilizer angle for the airplane with wings of 40° or 20° sweep at either altitude. The large trim change for the 60° swept wing was principally due to the longitudinal location of the wing used in the tests. The variation with Mach number of stabilizer angle required for trim was stable over the range tested for the three sweep angles at both altitudes, except for the 20° configuration which showed a slightly unstable variation above a Mach number of about 0.9 at both altitudes.

(4) For all three swept wings tested, the values of the rate of change of downwash angle with angle of attack increased gradually with increasing Mach number, maximum values being reached at progressively higher Mach numbers (all less than 1.00) in the order of increasing sweepback, after which there was a decrease with further increase in Mach number.

Langley Aeronautical Laboratory,
National Advisory Committee for Aeronautics,
Langley Field, Va.

REFERENCES

1. Silsby, Norman S., Morris, Garland J., and Kennedy, Robert M.: Longitudinal Characteristics at Mach Number of 1.24 of $\frac{1}{30}$ - Scale Semispan Model of Bell X-5 Variable-Sweep Airplane With Wing Swept Back 60° From Tests by NACA Wing-Flow Method. NACA RM L50E02a, 1950.

2. Morris, Garland J., Kennedy, Robert M., and Silsby, Norman S.: The Effect of Sweepback on the Longitudinal Characteristics at a Mach Number of 1.24 of a $\frac{1}{30}$ - Scale Semispan Model of the Bell X-5 Airplane From Tests by the NACA Wing-Flow Method. NACA RM L50I28, 1950.

3. Sawyer, Richard H., Kennedy, Robert M., and Morris, Garland J.: Longitudinal-Control Effectiveness and Downwash Characteristics at a Mach Number of 1.24 of a $\frac{1}{30}$ - Scale Semispan Model of the Bell X-5 Airplane As Determined by the NACA Wing-Flow Method. NACA RM L50K15, 1951.

4. Kennedy, Robert M.: Effects of a Fuselage Flap Dive Brake on the Aerodynamic Characteristics of $\frac{1}{30}$ - Scale Semispan Model of the Bell X-5 Variable-Sweep Airplane at a Mach Number 1.24 As Determined by the NACA Wing-Flow Method. NACA RM L50L11a, 1951.

5. Silsby, Norman S., and Morris, Garland J.: Investigation of the Distribution of Lift, Drag, and Pitching Moment Between the Wing and Fuselage of a $\frac{1}{30}$ - Scale Semispan Model of the Bell X-5 Airplane at a Mach Number of 1.24 by the NACA Wing-Flow Method. NACA RM L51K27, 1952.

6. Kolnick, Joseph J. and Kennedy, Robert M.: The Effects of Sweepback on the Longitudinal Characteristics of a $\frac{1}{30}$ - Scale Semispan Model of the Bell X-5 Airplane As Determined From NACA Wing-Flow Tests at Transonic Speeds. NACA RM L52I23, 1952.

7. Johnson, Harold I.: Measurements of Aerodynamic Characteristics of a 35° Sweptback NACA 65-009 Airfoil Model With a $\frac{1}{4}$ - Chord Plain Flap by the NACA Wing-Flow Method. NACA RM L7F13, 1947.

TABLE I

GEOMETRIC CHARACTERISTICS OF $\frac{1}{30}$ - SCALE SEMISPAN MODEL

OF BELL X-5 AIRPLANE

Wing dimensions:			
Sweepback angle, deg	20	40	60
Semispan, in.	6.18	5.31	3.88
Mean aerodynamic chord, in.	2.96	3.10	3.64
Chord at tip, in.	1.84	1.84	1.84
Chord at plane of symmetry	4.50	4.40	4.25
Area (semispan), sq in.	15.84	14.97	13.79
Aspect ratio	4.82	3.77	2.18
Dihedral (chord plane), deg	0	0	0
Incidence (chord plane), deg	0	0	0
Airfoil section (perpendicular to unswept 38.6-percent-chord line)			
Root	NACA $64_{(10)}$A011		
Tip	NACA $64_{(08)}$A008.6		
Horizontal tail:			
Section	NACA 64A006		
Semispan, in.	1.91		
Mean aerodynamic chord, in.	1.43		
Chord at tip, in.	0.72		
Chord at plane of symmetry, in.	1.95		
Area (semispan), sq in.	2.55		
Aspect ratio	2.86		
Height (above wing chord), in.	0.56		
Tail length			
From $0.35\bar{c}$ of 20° wing to $0.25\bar{c}_t$, in.	6.83		
From $0.35\bar{c}$ of 40° wing to $0.25\bar{c}_t$, in.	6.83		
From $0.26\bar{c}$ of 60° wing to $0.25\bar{c}_t$, in.	6.83		

TABLE II

INDEX TO FIGURES

Quantity	Configuration		Figure
	Λ, deg	i_t, deg	
C_m', C_D', and α against M_w	60	0 -4 -6 Tail off	7(a) 7(b) 7(c) 7(d)
C_m, C_D, and α against M_w	40	-6 Tail off	8(a) 8(b)
C_m, C_D, and α against M_w	20	-6 Tail off	9(a) 9(b)
C_L' against α at M_w = 0.75, 0.85, 0.95, and 1.00	60	0 -2 -4 -6 Tail off	10(a)
	40	-2 -6 Tail off	10(b)
	20	-2 -6 Tail off	10(c)
C_m' against C_L' at M_w = 0.75, 0.85, 0.95, and 1.00	60	0 -2 -4 -6 Tail off	11(a)
	40	-2 -6 Tail off	11(b)
	20	-2 -6 Tail off	11(c)
C_L' against C_D' at M_w = 0.75, 0.85, 0.95 and 1.00	60	0 -2 -4 -6 Tail off	12(a)
	40	-2 -6 Tail off	12(b)
	20	-2 -6 Tail off	12(c)

TABLE II

INDEX TO FIGURES - Concluded

Quantity		Configuration		Figure
		Λ, deg	i_t, deg	
$\frac{\partial C_m'}{\partial C_L'}$ against M_w	$C_L' = 0$	60	-2 -6 Tail off	13(a)
		40	-2 -6 Tail off	
		20	-2 -6 Tail off	
	$C_L' = 0.4$	60	-2 -6 Tail off	13(b)
		40	-2 -6 Tail off	
		20	-2 -6 Tail off	
α at start of pitch-up against M_w		60 40 20	-------- -------- --------	14
C_m' against i_t for various α	$M_w = 0.75$	60, 40, and 20	--------	15(a)
	$M_w = 0.85$	60, 40, and 20	--------	15(b)
	$M_w = 0.95$	60, 40, and 20	--------	15(c)
	$M_w = 1.00$	60, 40, and 20	--------	15(d)
$\frac{\partial C_m'}{\partial i_t}$ against M_w for various α		60	--------	16
$i_{t_{Trim}}$ against M_w		60, 40, and 20	--------	17
$\frac{d\epsilon}{d\alpha}$ against M_w		60, 40, and 20	--------	18

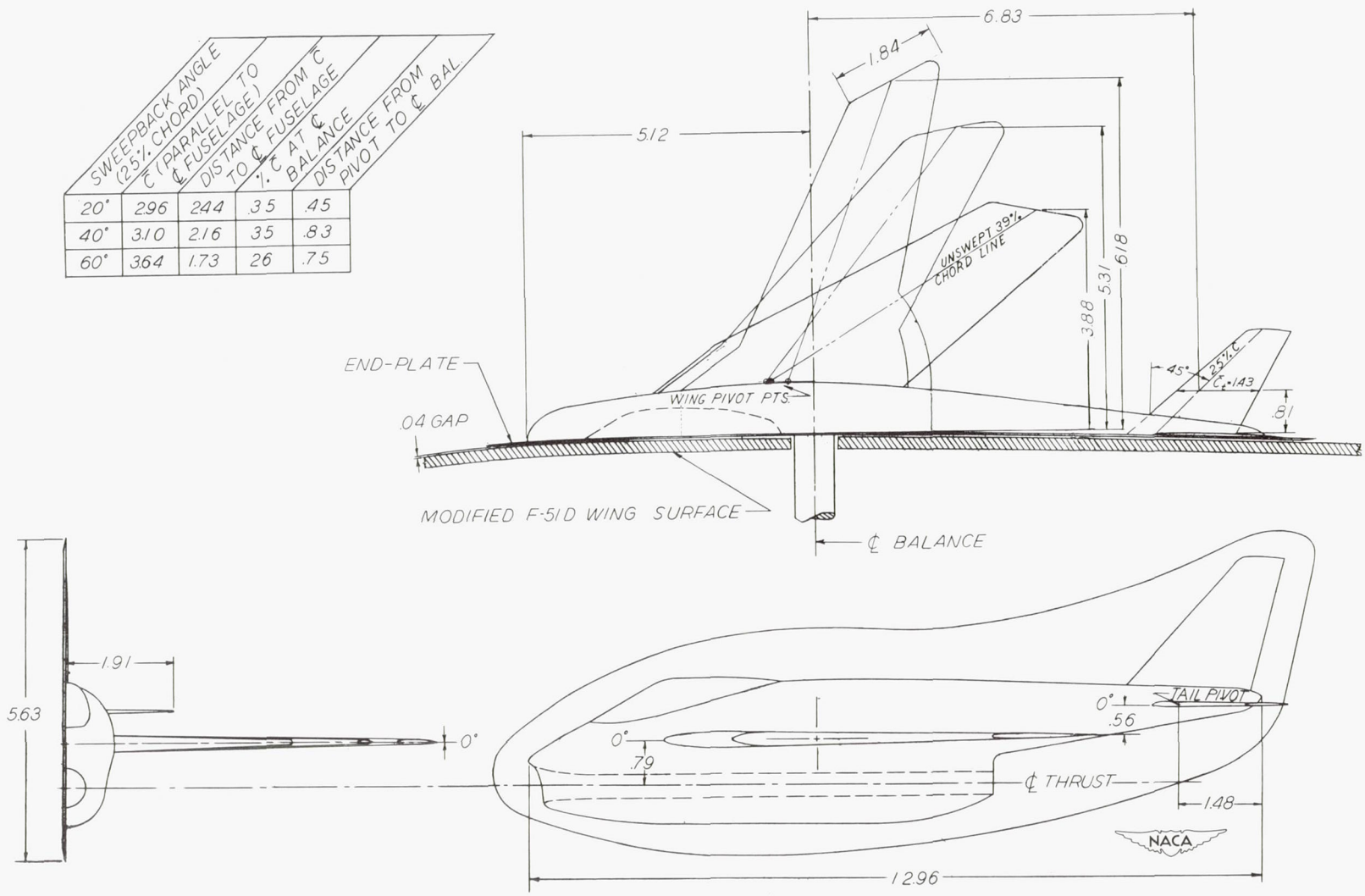

Figure 1.- Details of the semispan model of Bell X-5 airplane.
(All dimensions are in inches.)

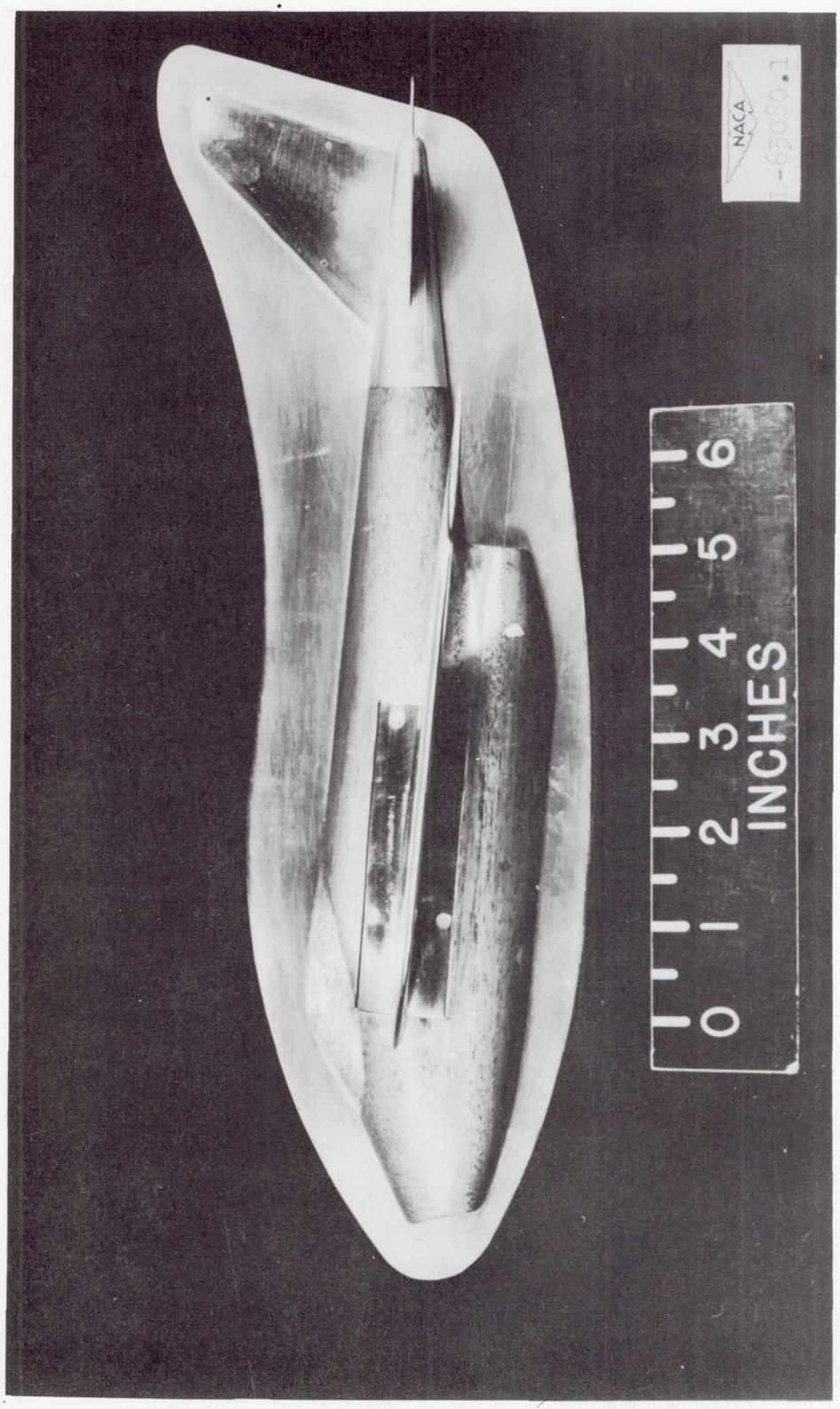

Figure 2.- Side view of semispan wing-flow model of the Bell X-5 airplane.

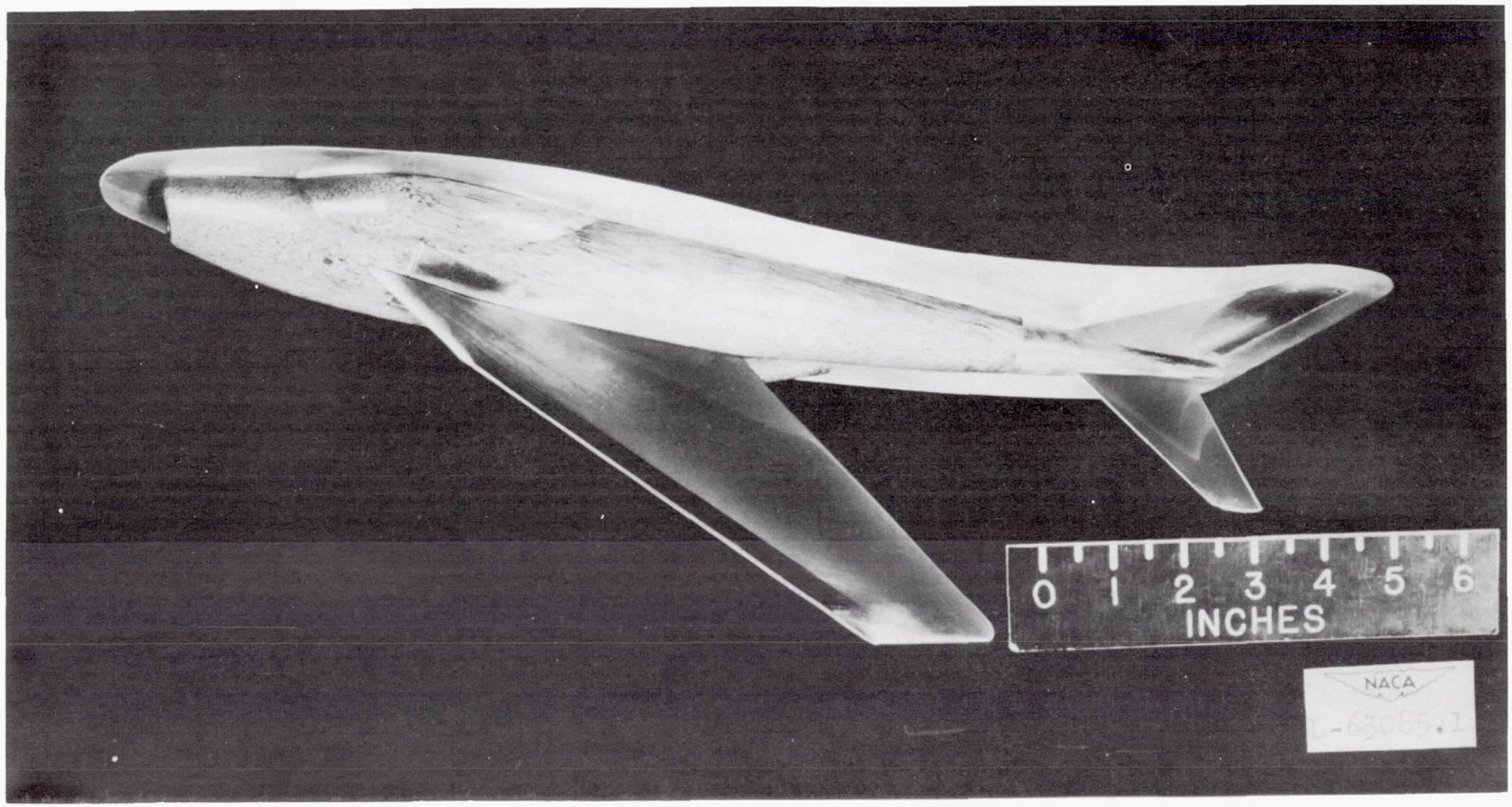

(a) 60° sweptback wing.

Figure 3.- Photographs of Bell X-5 semispan model equipped with various sweptback wings.

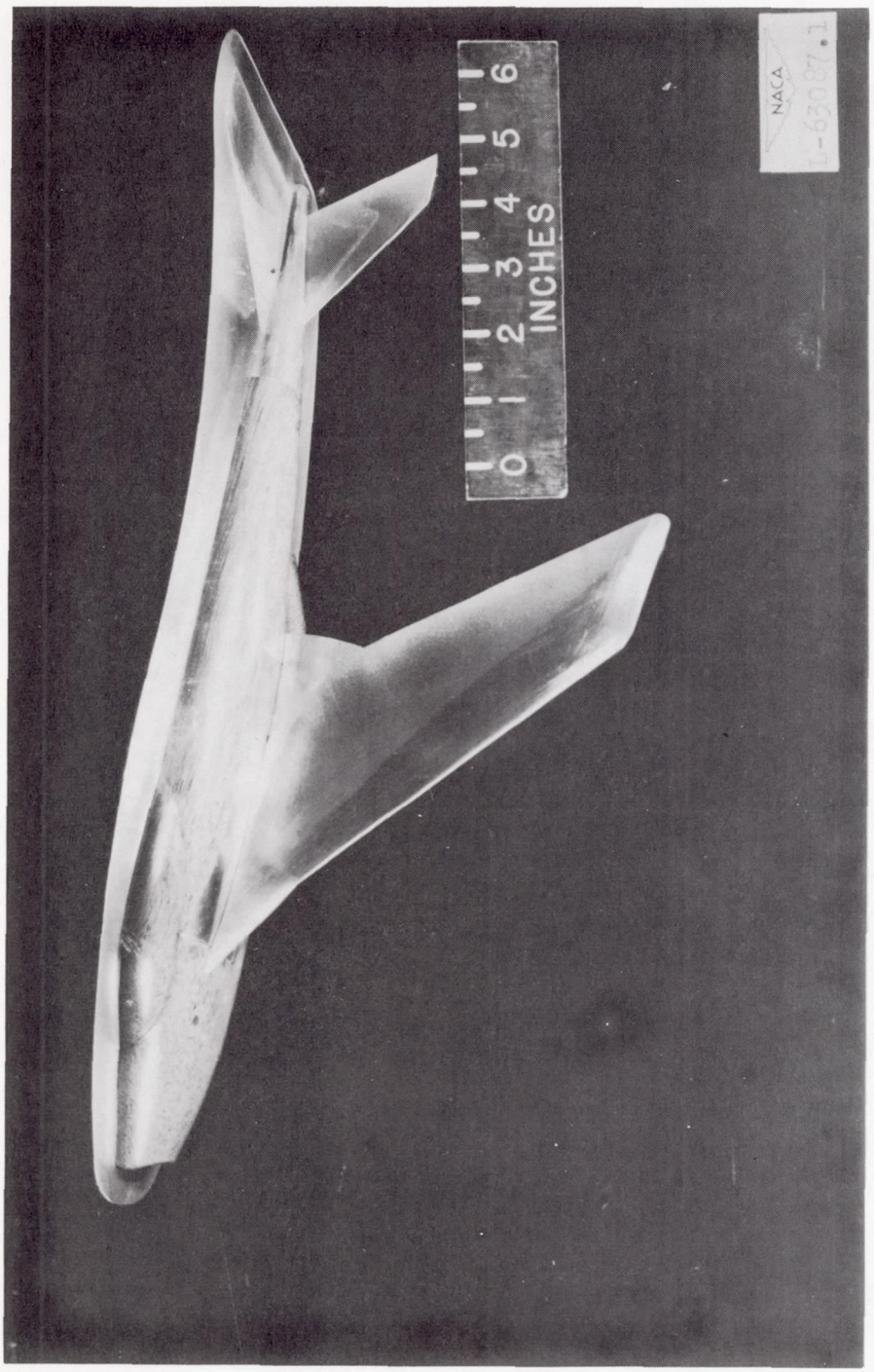

(b) 40° sweptback wing.

Figure 3.- Continued.

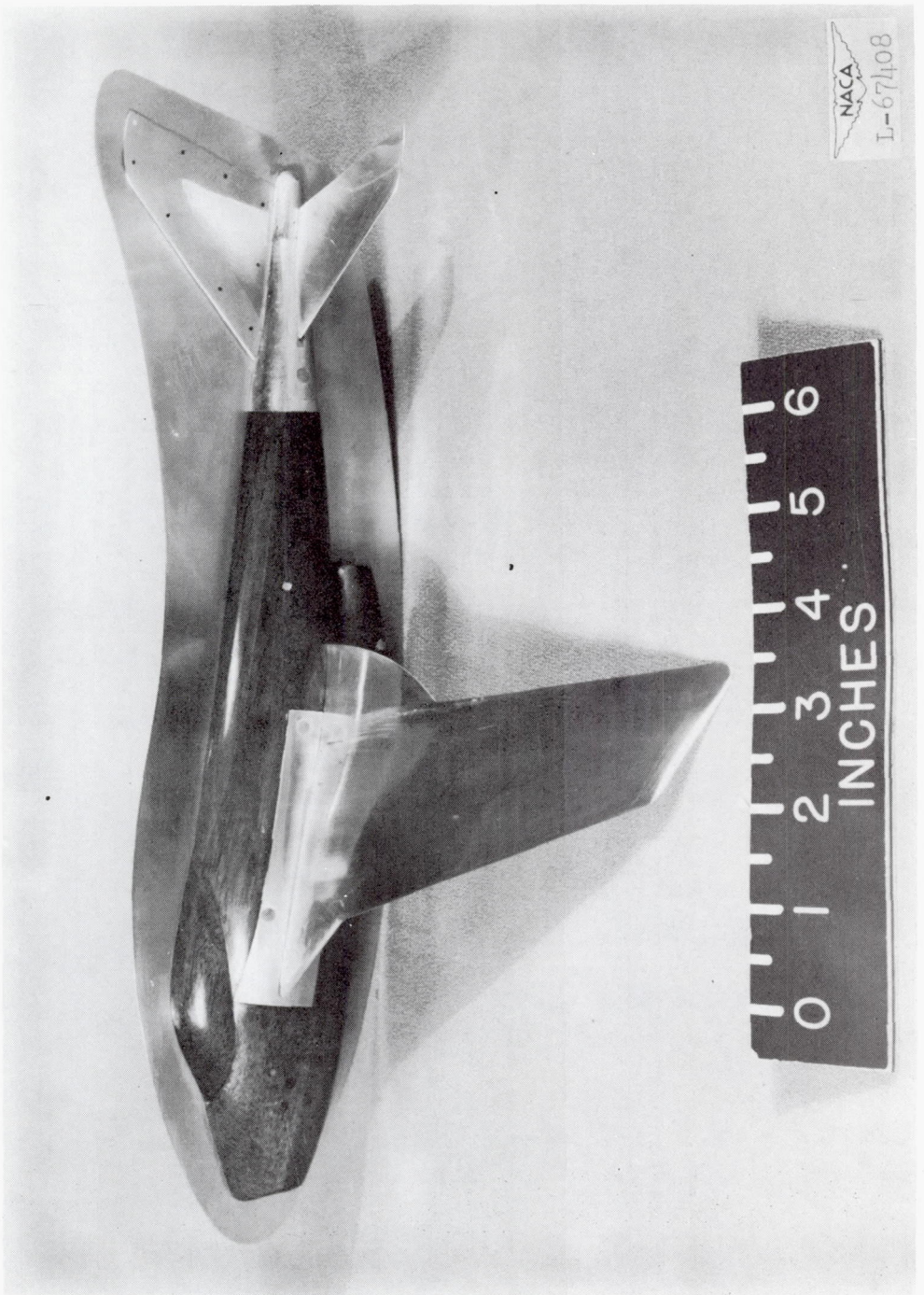

(c) 20° sweptback wing.

Figure 3.- Concluded.

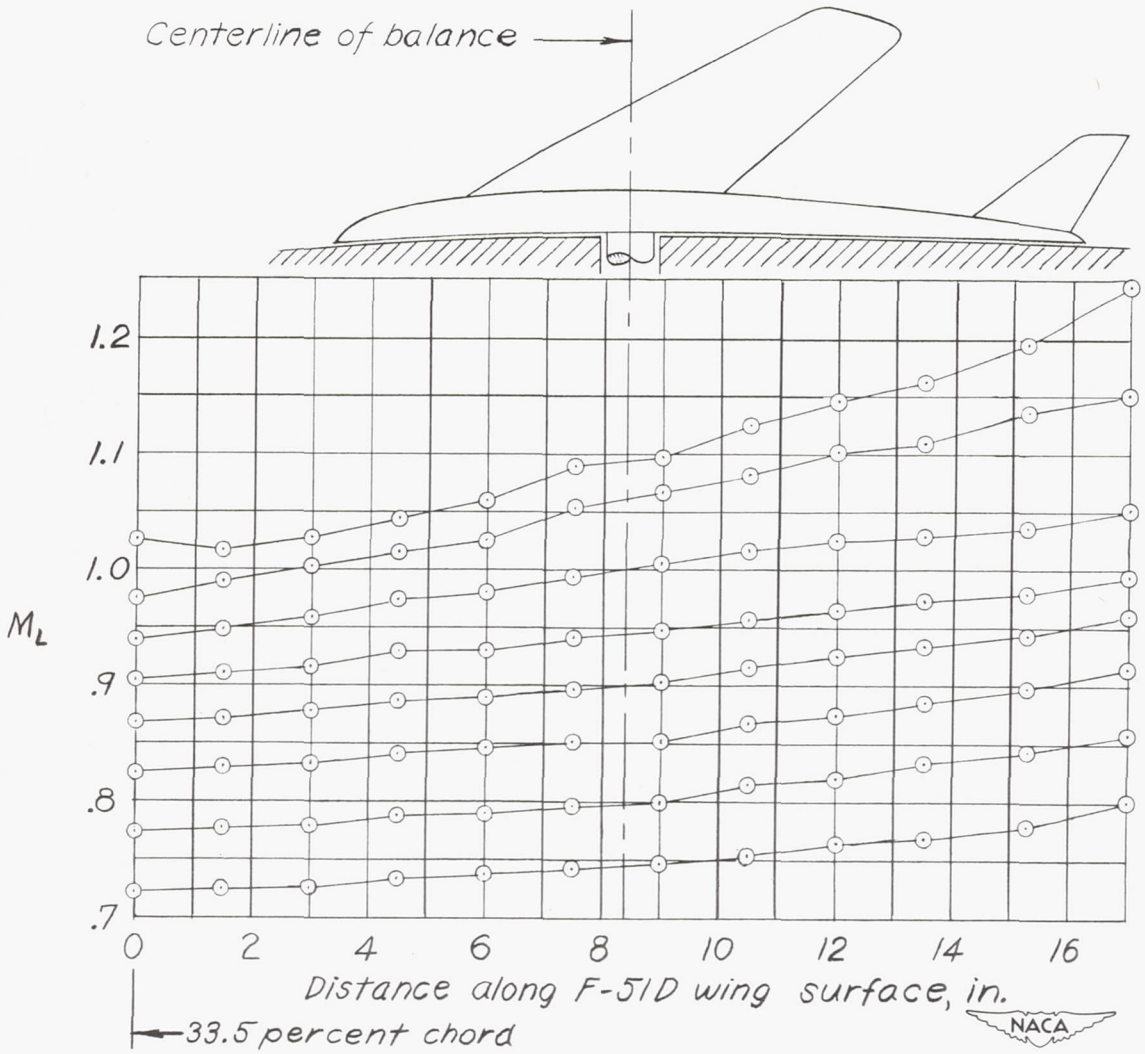

Figure 4.- Typical chordwise local Mach number variation measured at surface of test section. Chordwise location of model also shown.

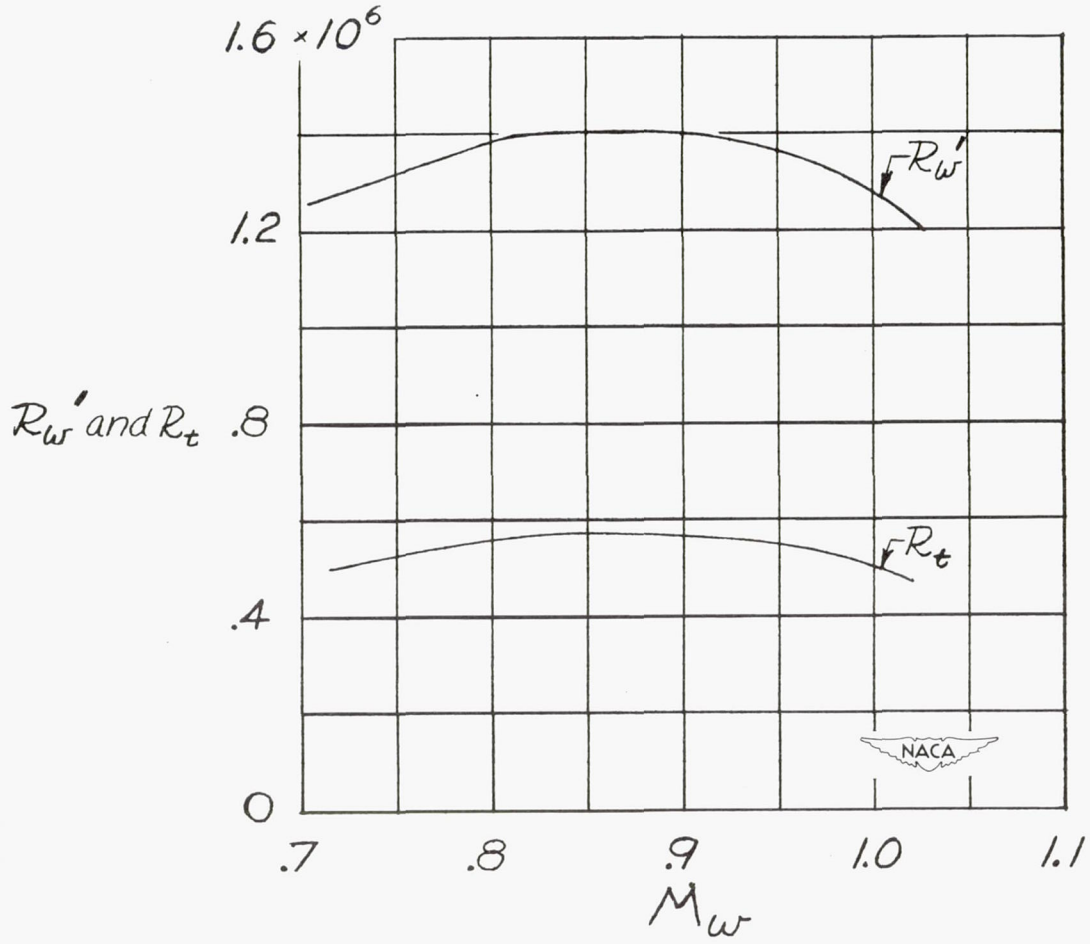

Figure 5.- Variation of Reynolds number of 60° sweptback wing R_w' and Reynolds number of tail R_t with Mach number at the wing M_w.

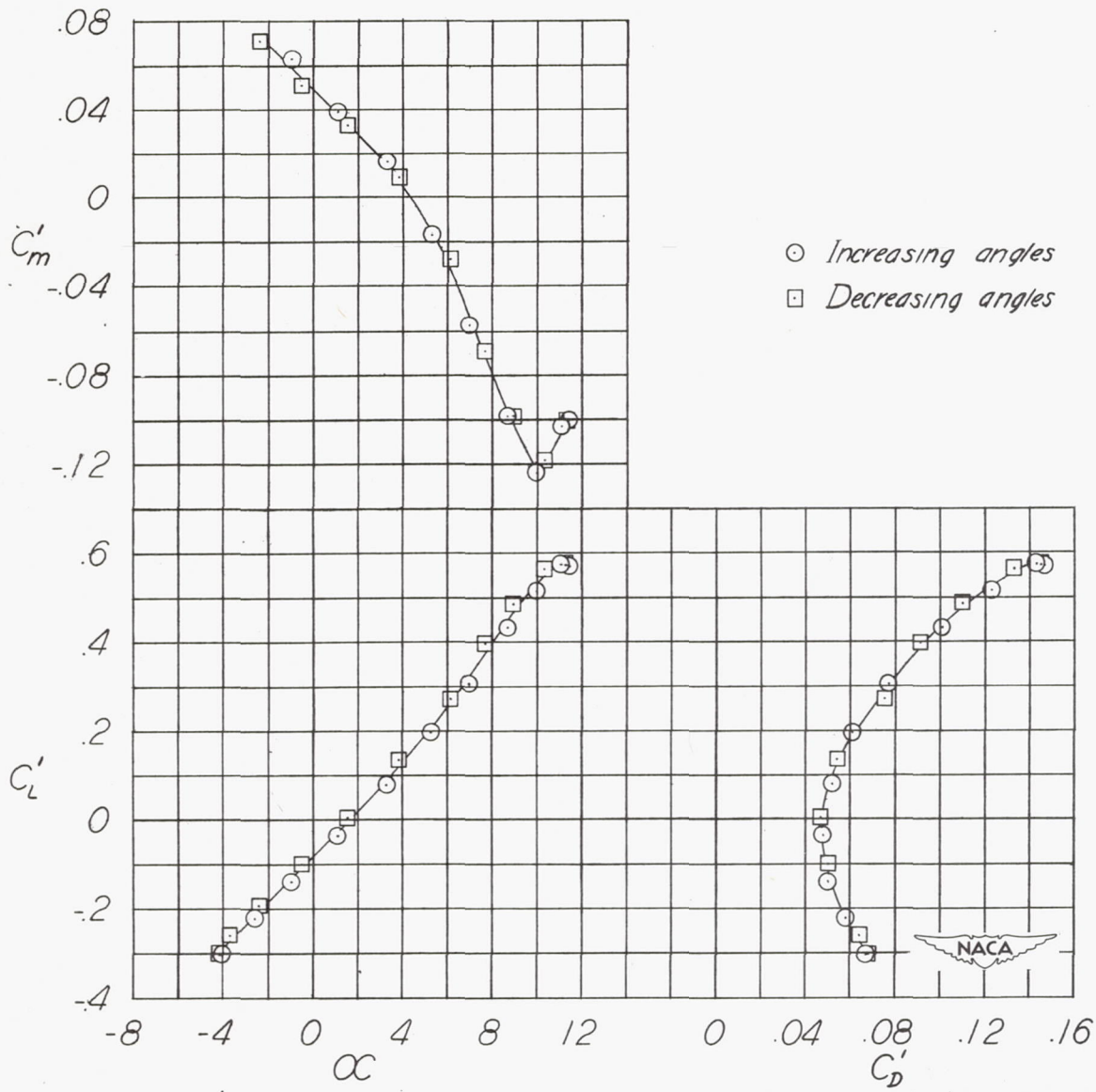

Figure 6.- Sample data for semispan model of Bell X-5 airplane with 60° sweptback wing and tail incidence of -4°. M = 0.856.

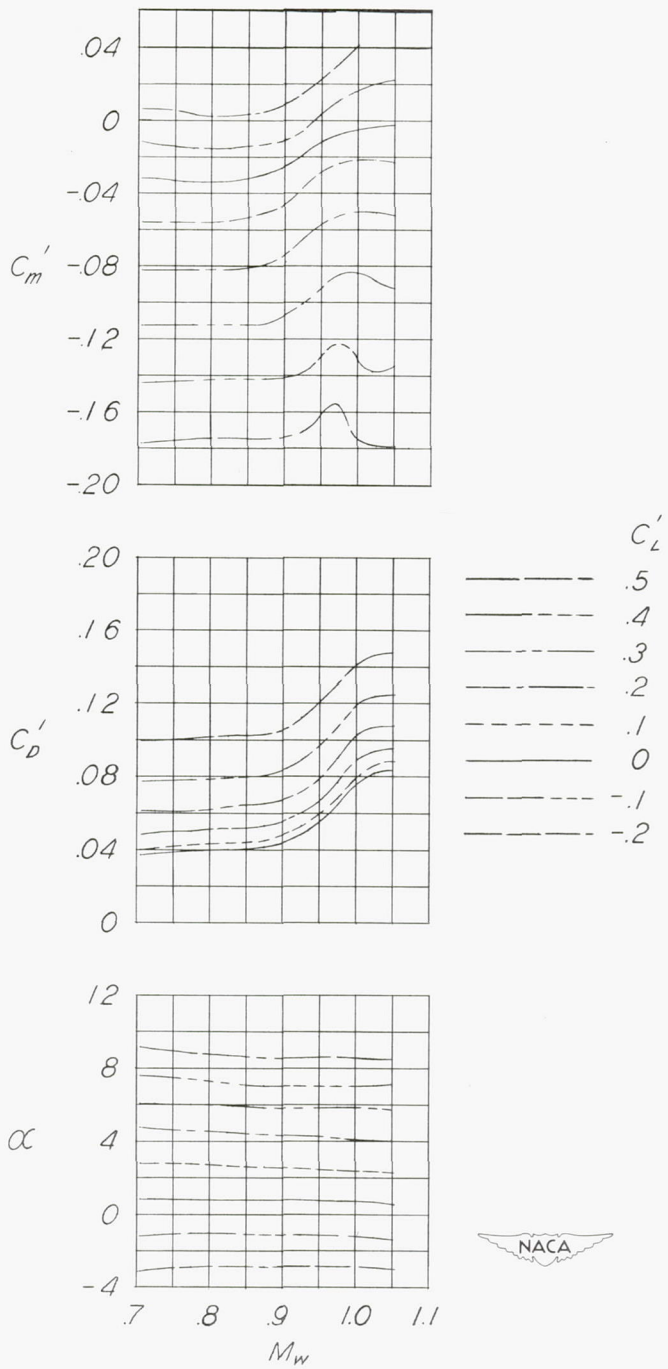

(a) $i_t = 0^\circ$.

Figure 7.- Variation with Mach number of C_m', C_D', and α for various lift coefficients for semispan model of Bell X-5 airplane with 60° sweptback wing. (Coefficients based on 60° sweptback-wing dimensions.)

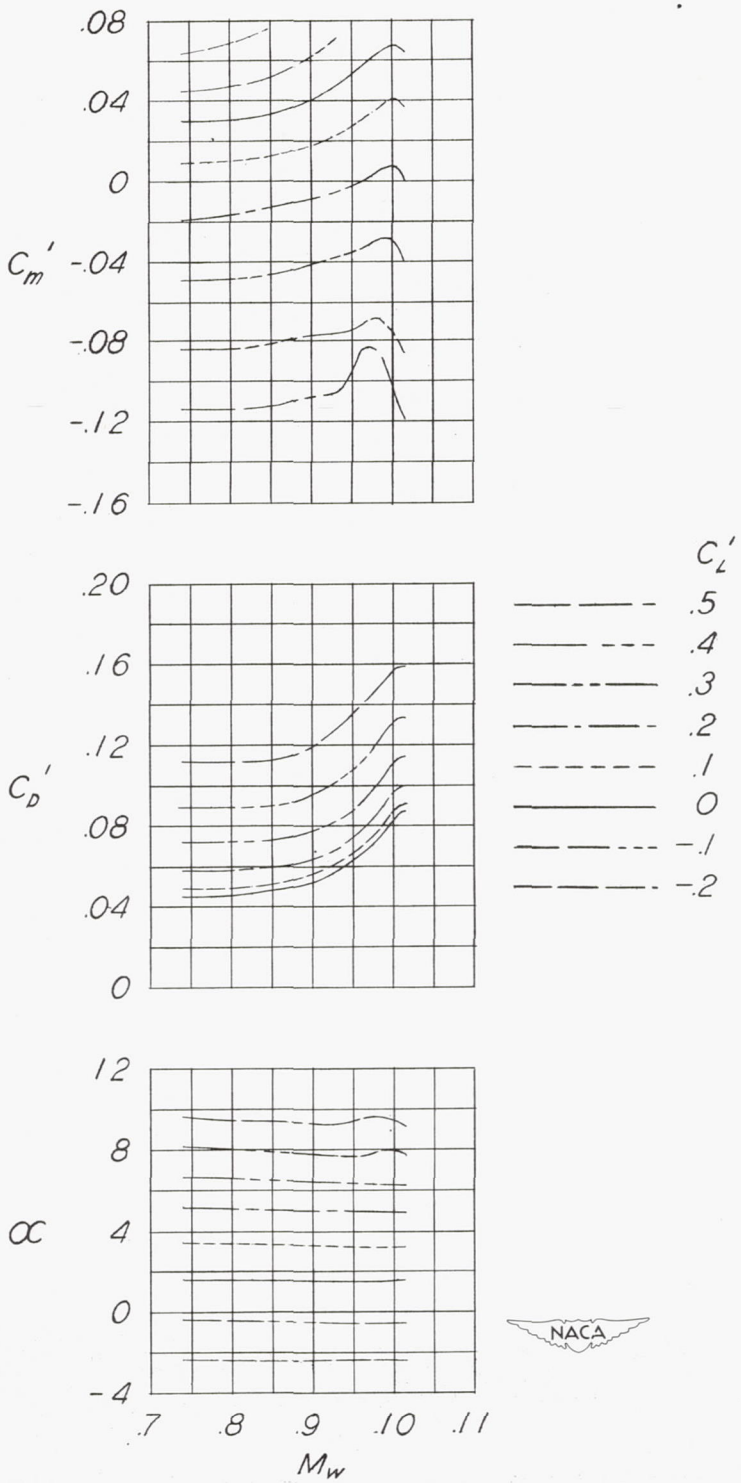

(b) $i_t = -4°$.

Figure 7.- Continued.

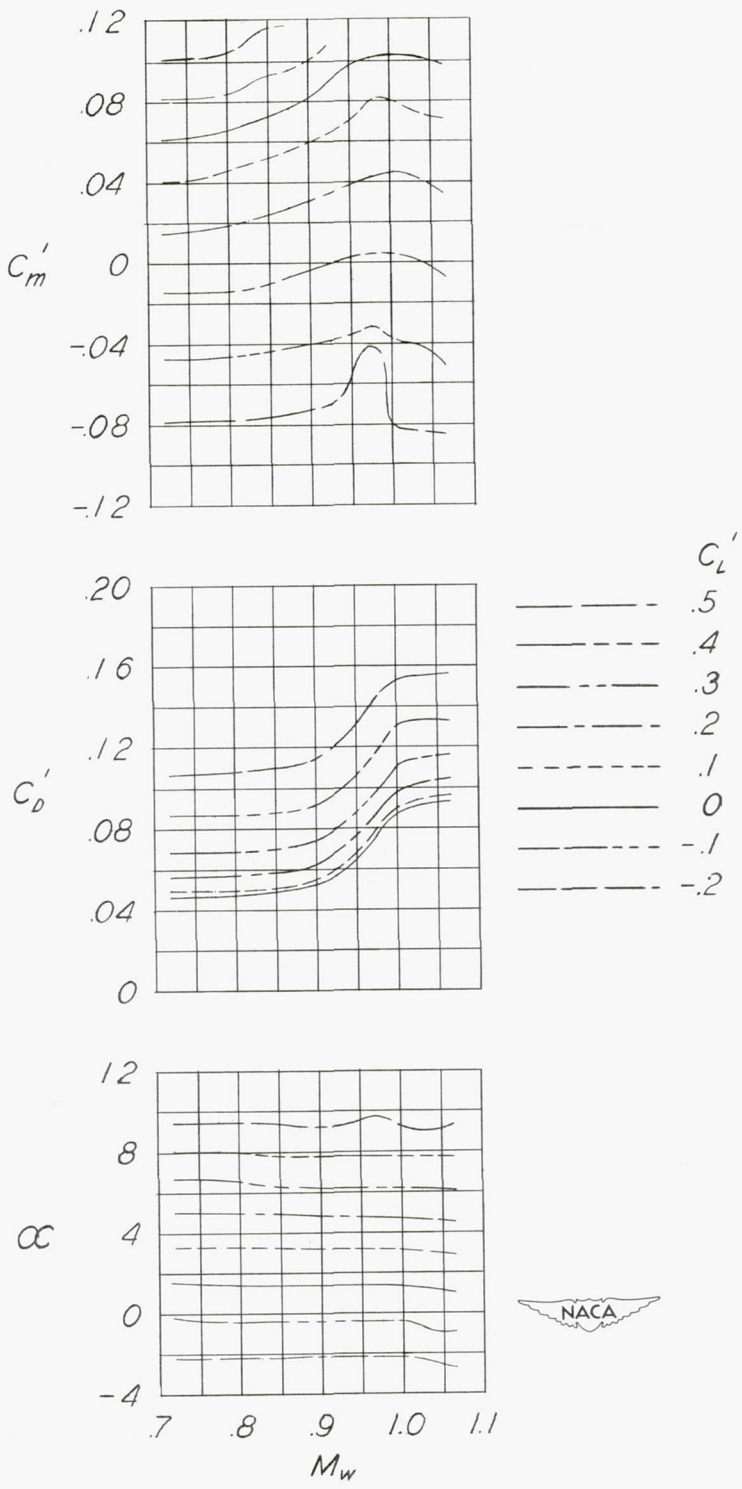

(c) $i_t = -6°$.

Figure 7.- Continued.

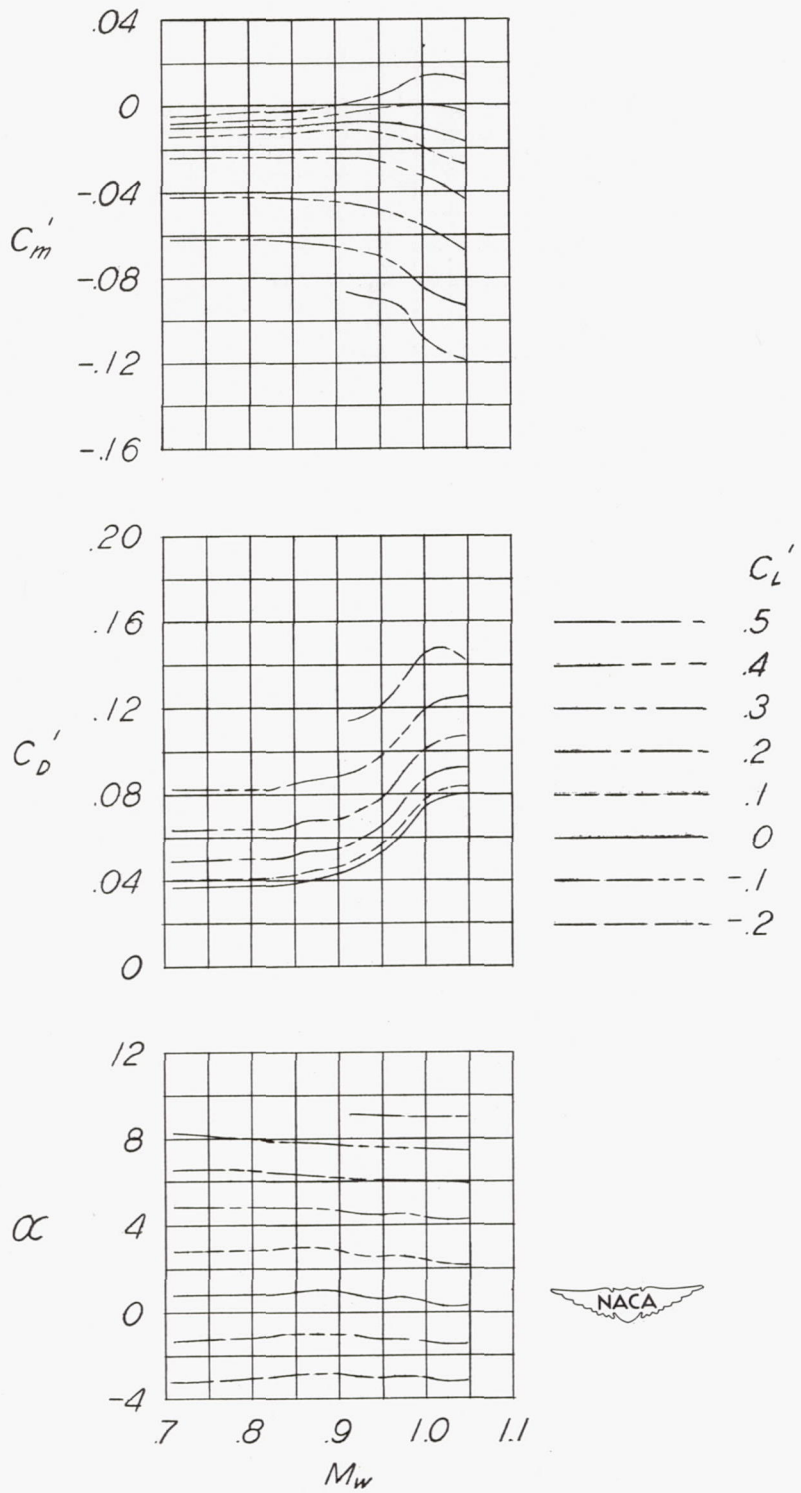

(d) Tail off.

Figure 7.- Concluded.

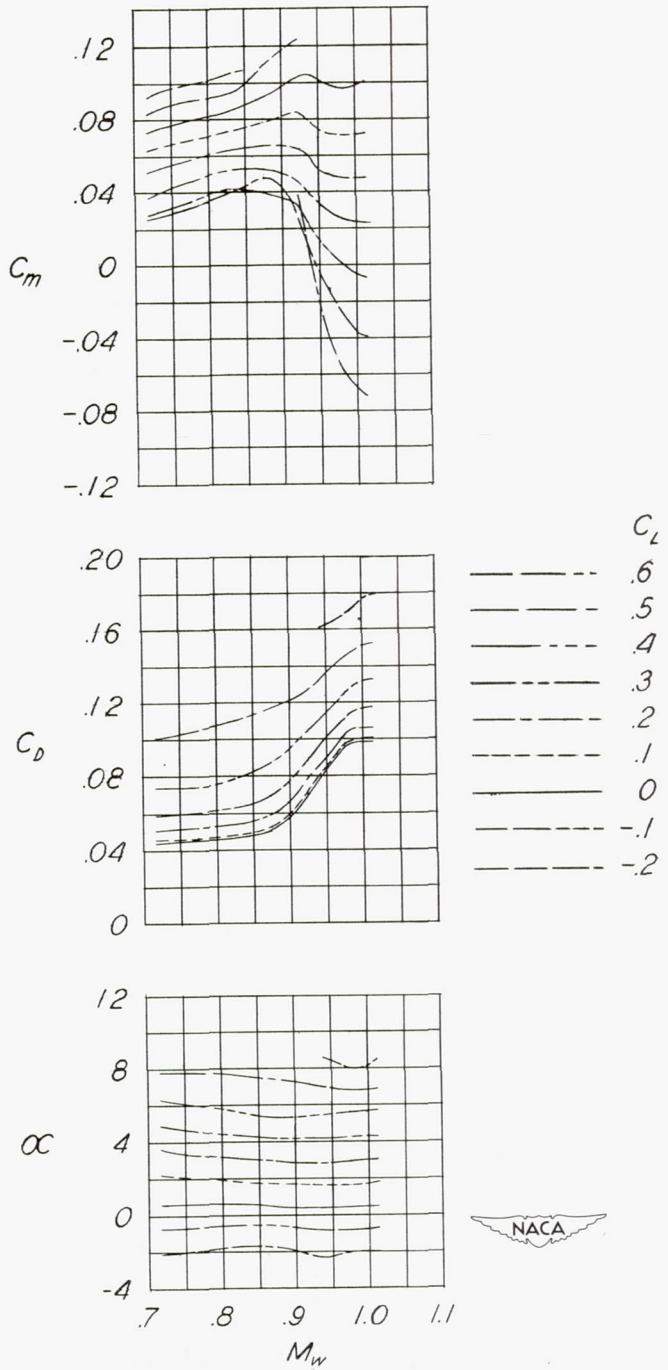

(a) $i_t = -6°$.

Figure 8.- Variation with Mach number of C_m, C_D, and α for various lift coefficients for semispan model of Bell X-5 airplane with 40° sweptback wing. (Coefficients based on 40° sweptback-wing dimensions.)

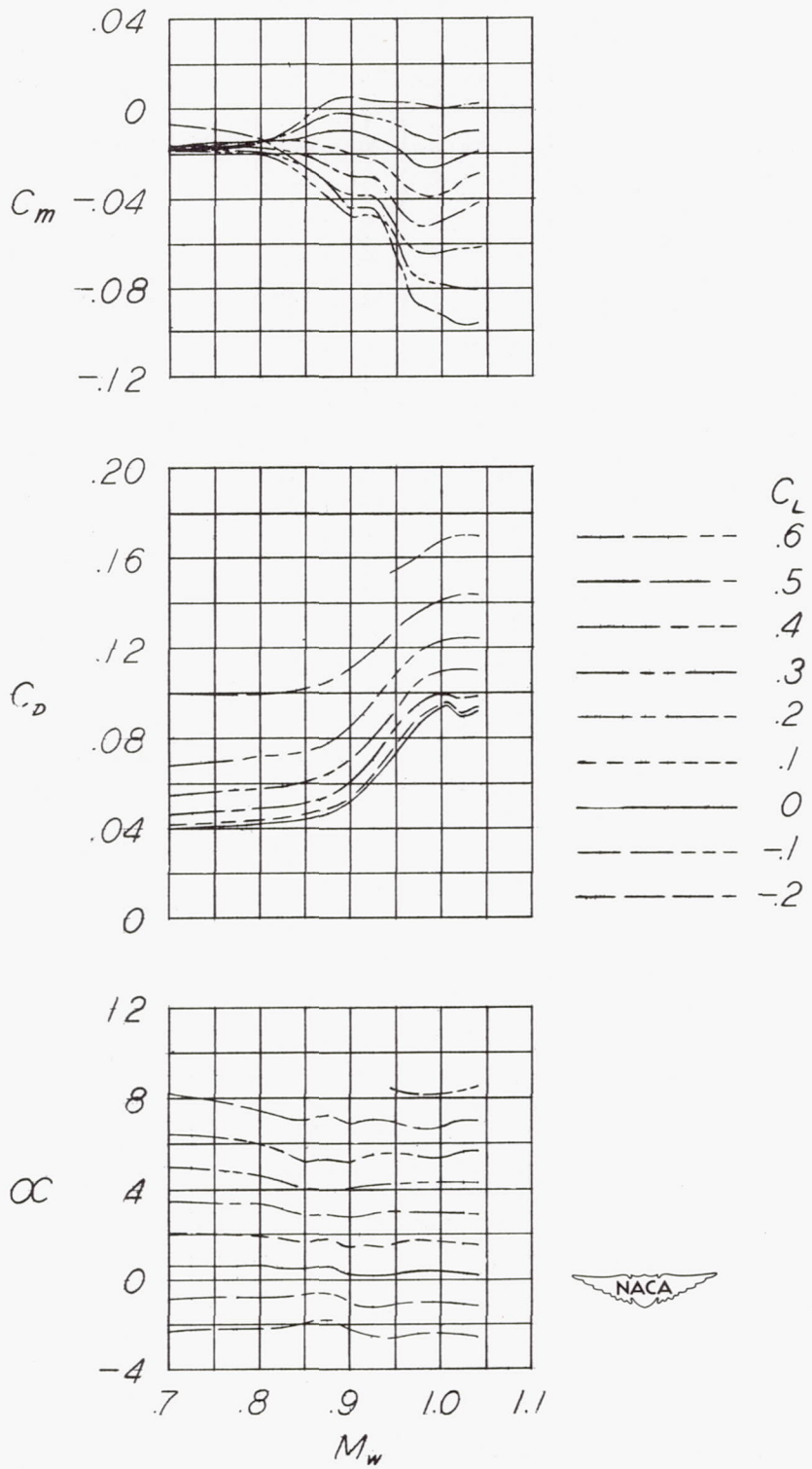

(b) Tail off.

Figure 8.- Concluded.

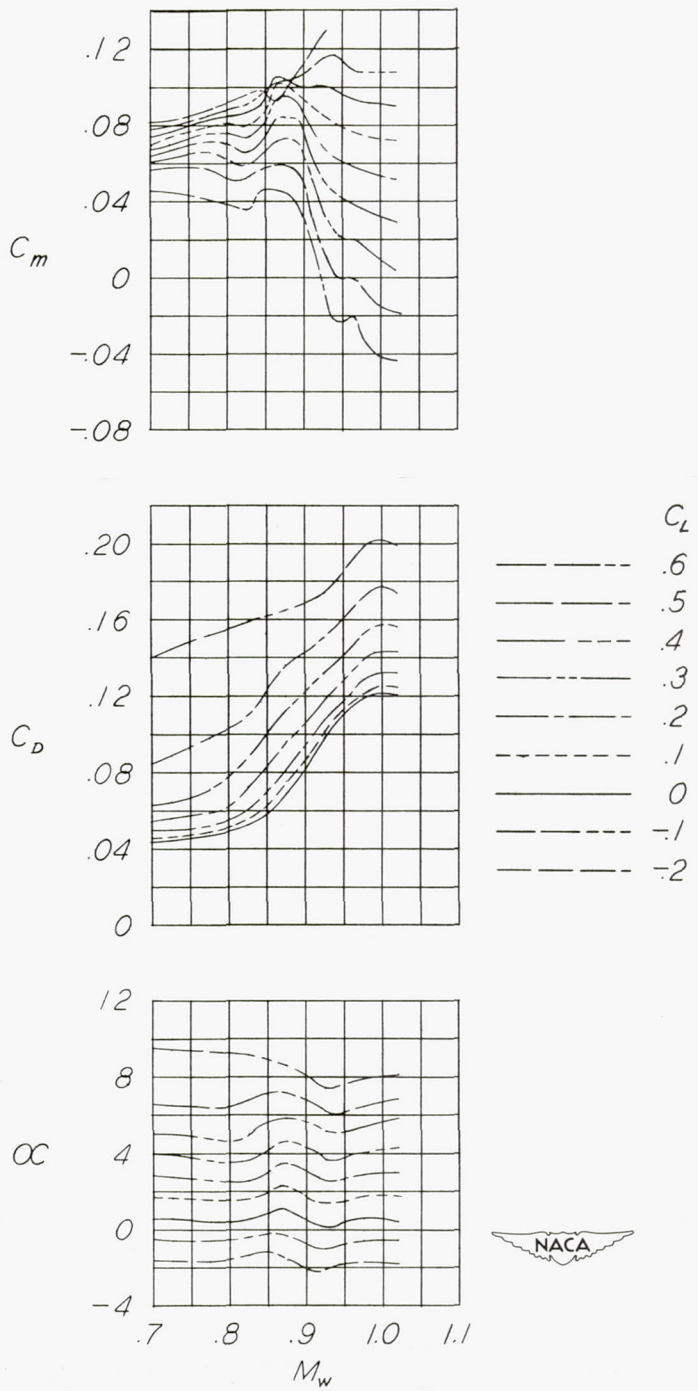

(a) $i_t = -6^\circ$.

Figure 9.- Variation with Mach number of C_m, C_D, and α for various lift coefficients for semispan model of Bell X-5 airplane with 20° sweptback wing. (Coefficients based on 20° sweptback-wing dimensions.)

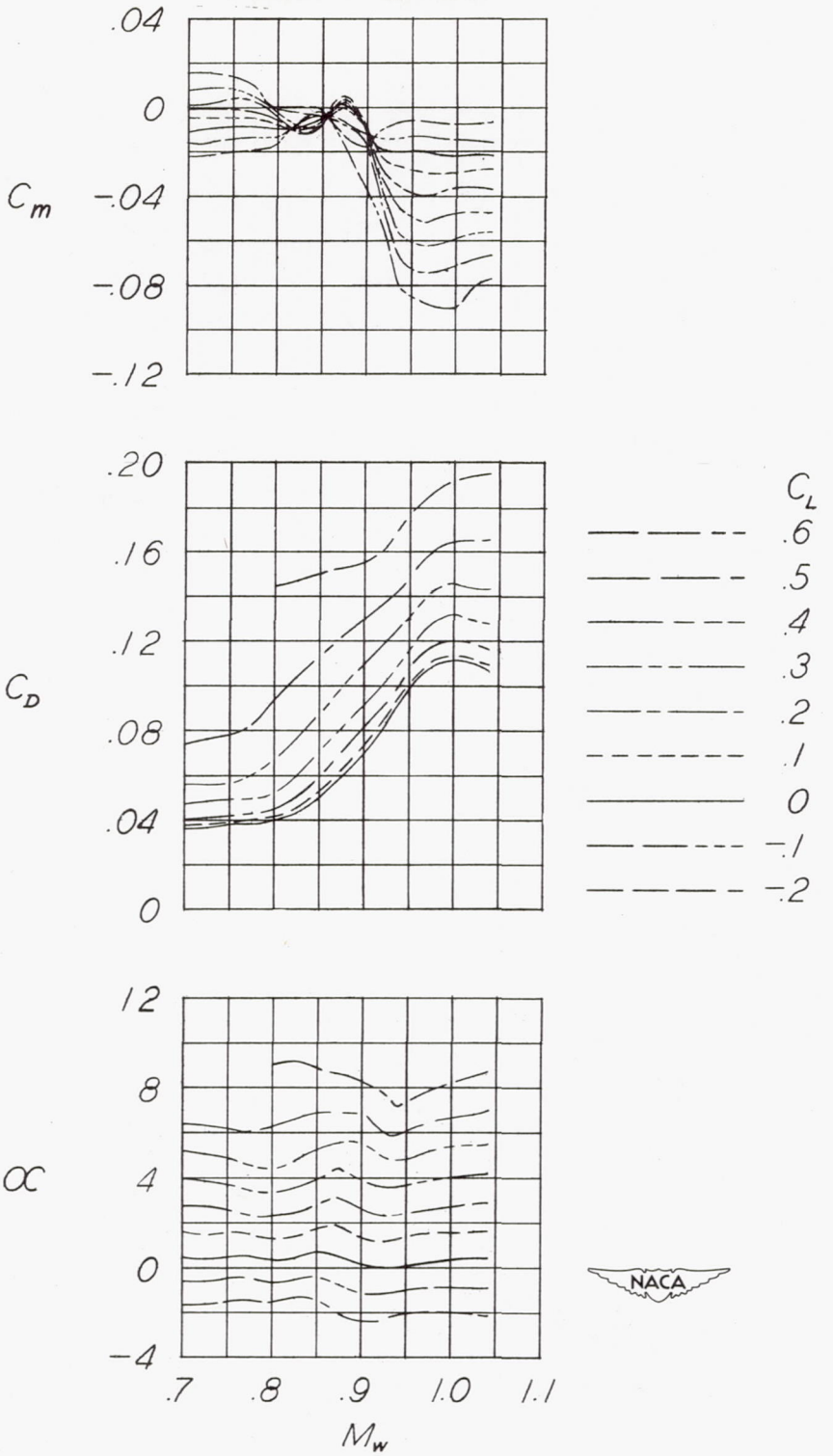

(b) Tail off.

Figure 9.- Concluded.

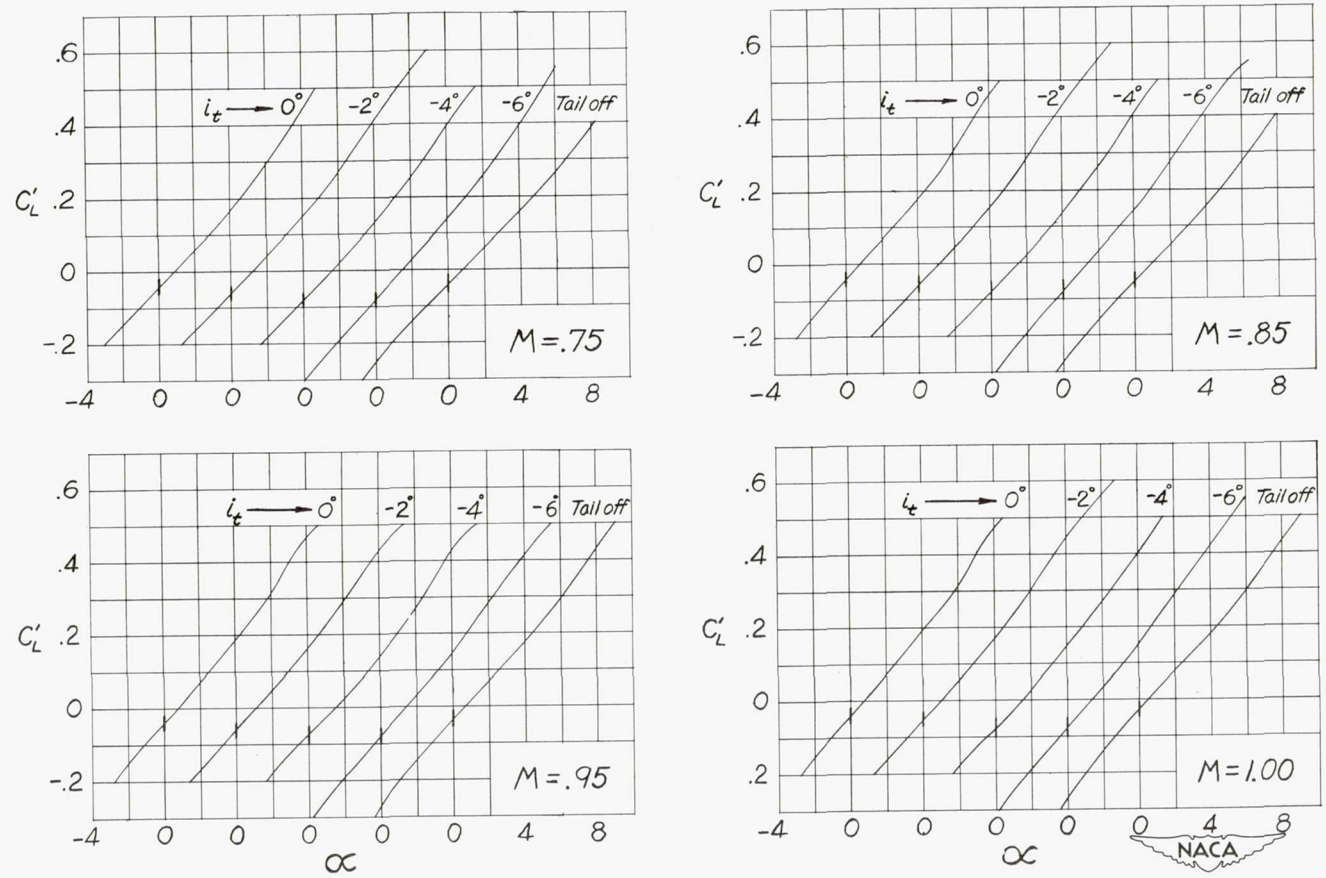

(a) $\Lambda = 60^\circ$.

Figure 10.- Variations of lift coefficient with angle of attack for several tail incidences and wing sweepback angles at several Mach numbers for semispan model of Bell X-5 airplane. Results from reference 6 ($i_t = -2^\circ$) are also shown. (Coefficients based on 60° sweptback-wing dimensions.)

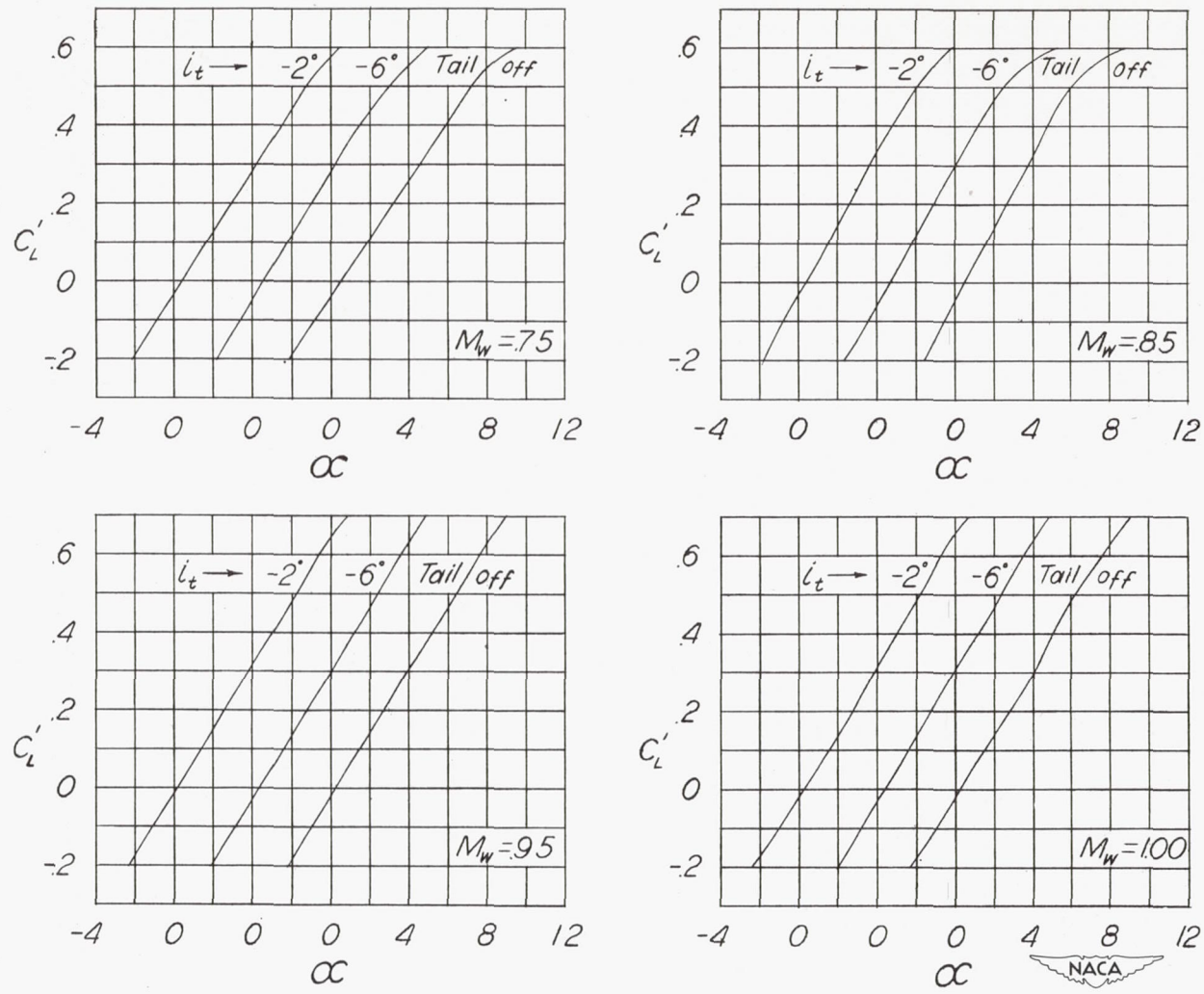

(b) $\Lambda = 40^\circ$.

Figure 10.- Continued.

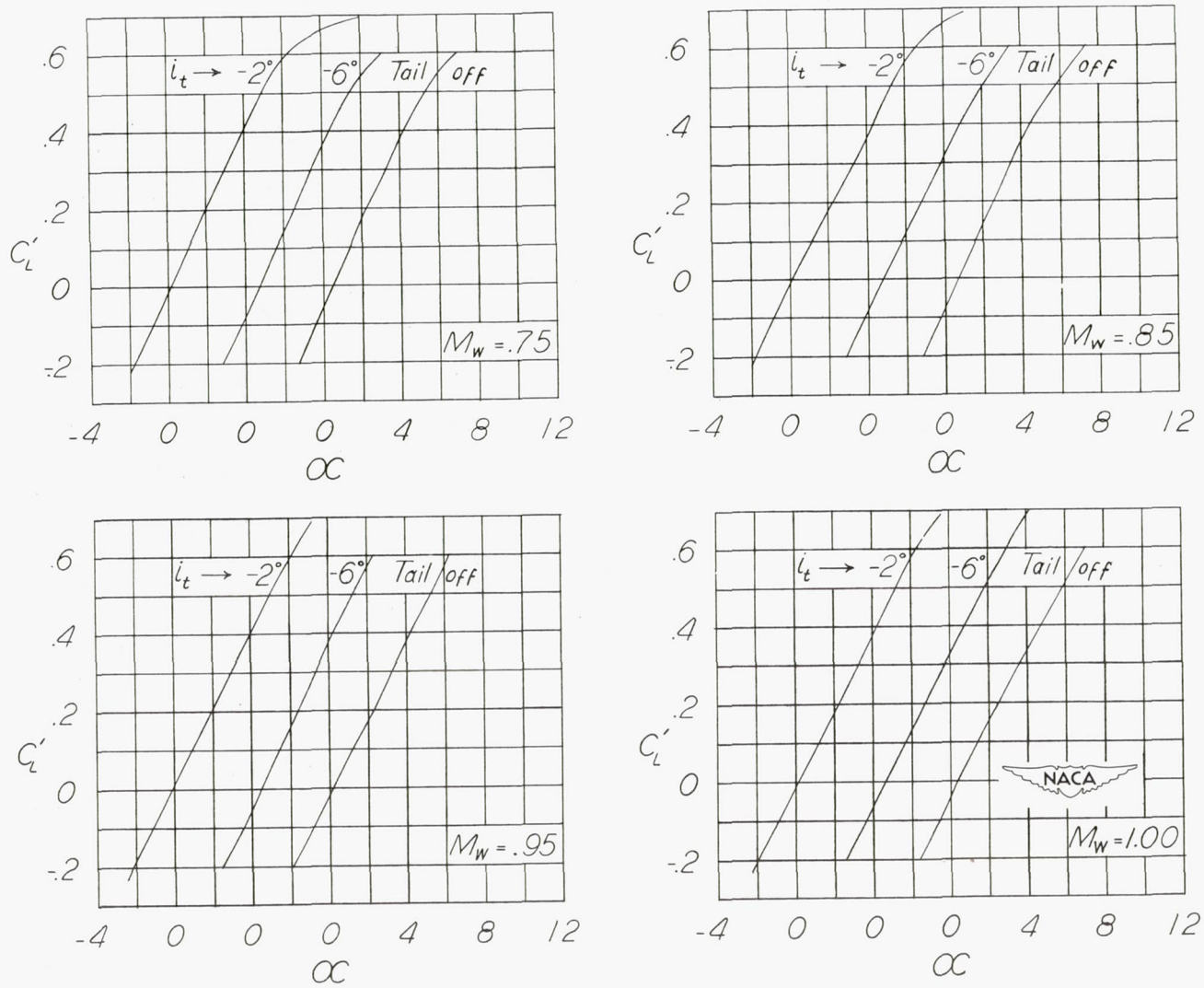

(c) $\Lambda = 20^\circ$.

Figure 10.- Concluded.

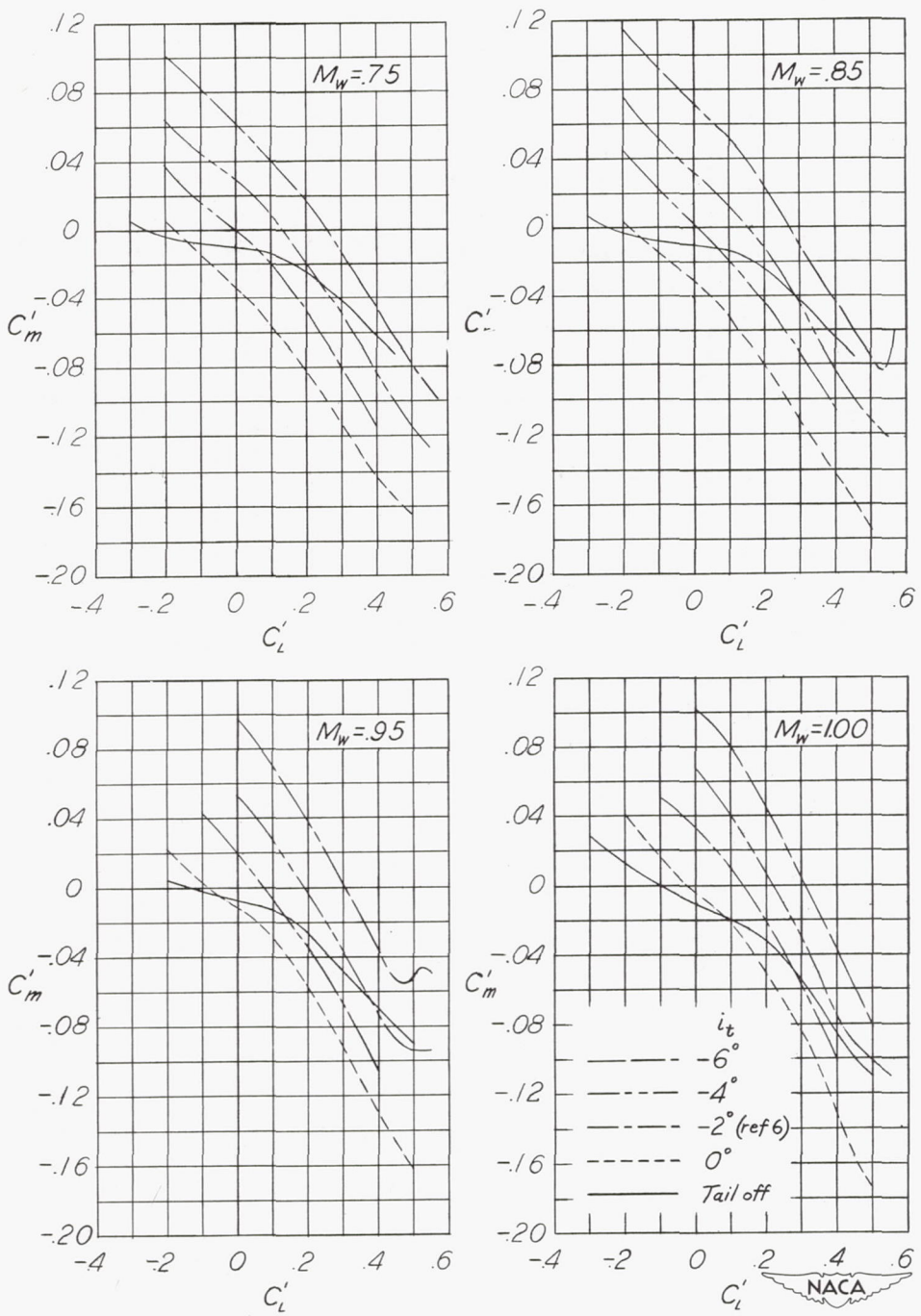

(a) $\Lambda = 60^\circ$.

Figure 11.- Variation of pitching-moment coefficient with lift coefficient for several tail incidences and wing sweepback angles at several Mach numbers for semispan model of Bell X-5 airplane. Results from reference 6 are also shown. (Coefficients based on 60° sweptback-wing dimensions.)

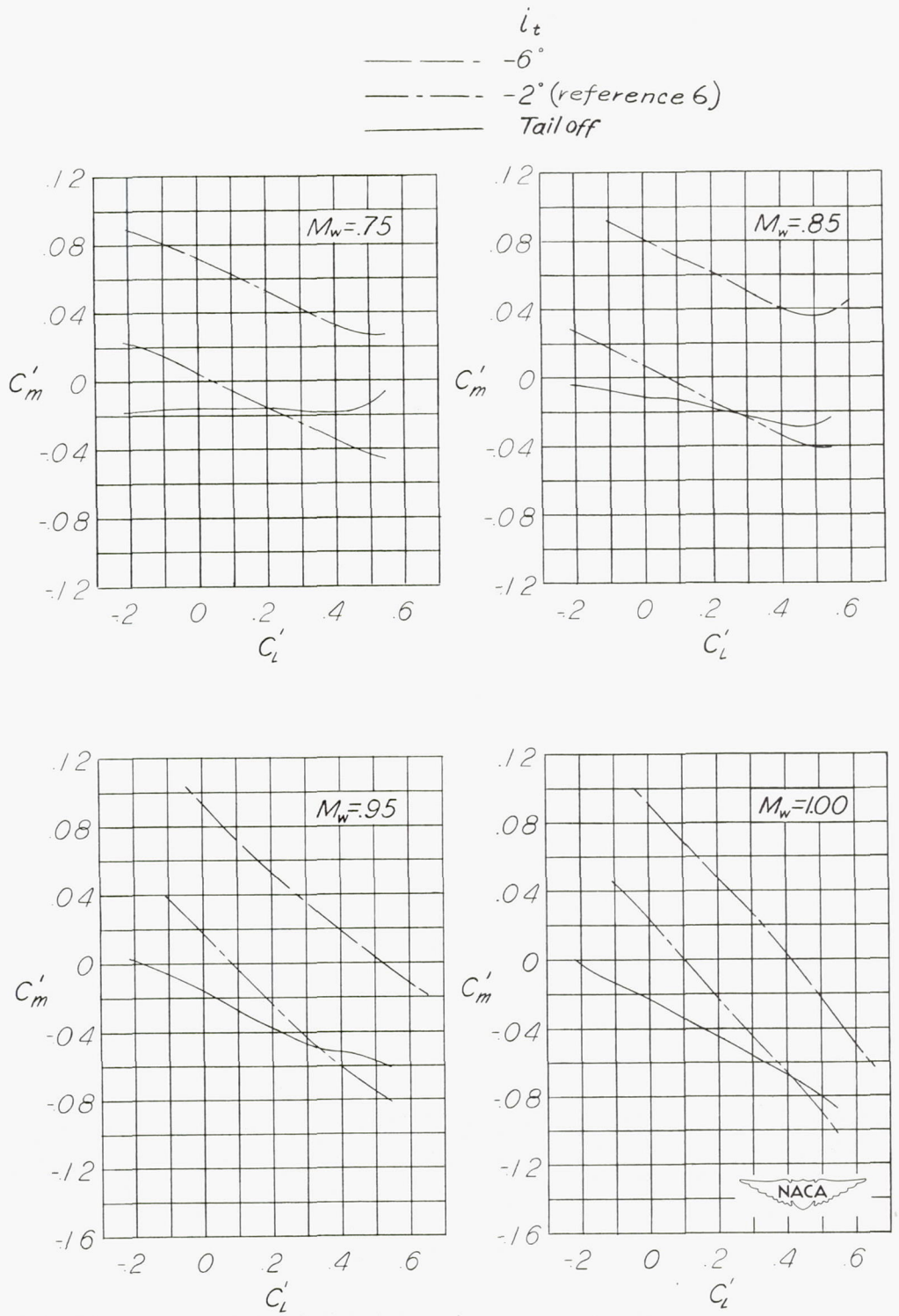

(b) $\Lambda = 40^{\circ}$.

Figure 11.- Continued.

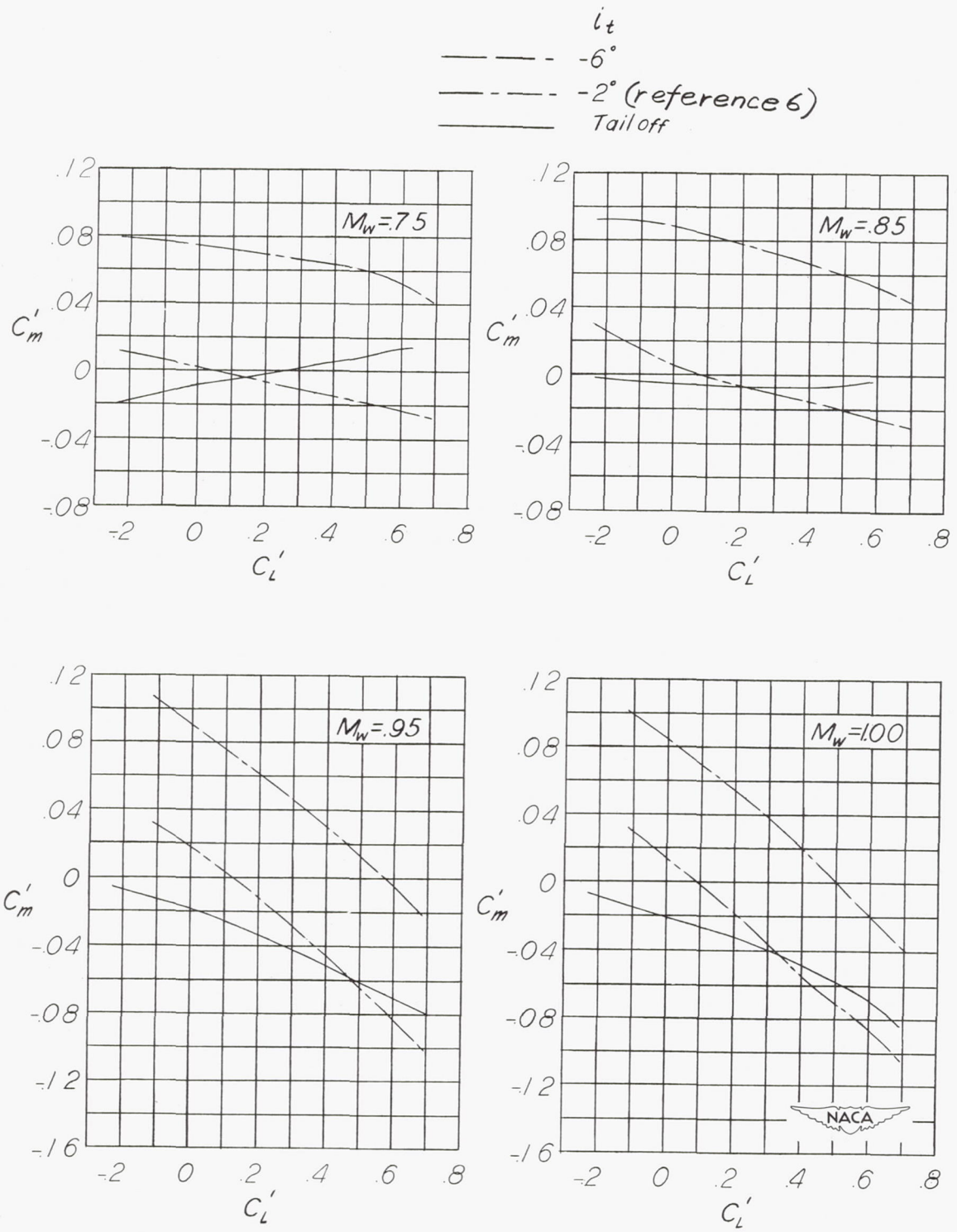

(c) $\Lambda = 20^{\circ}$.

Figure 11.- Concluded.

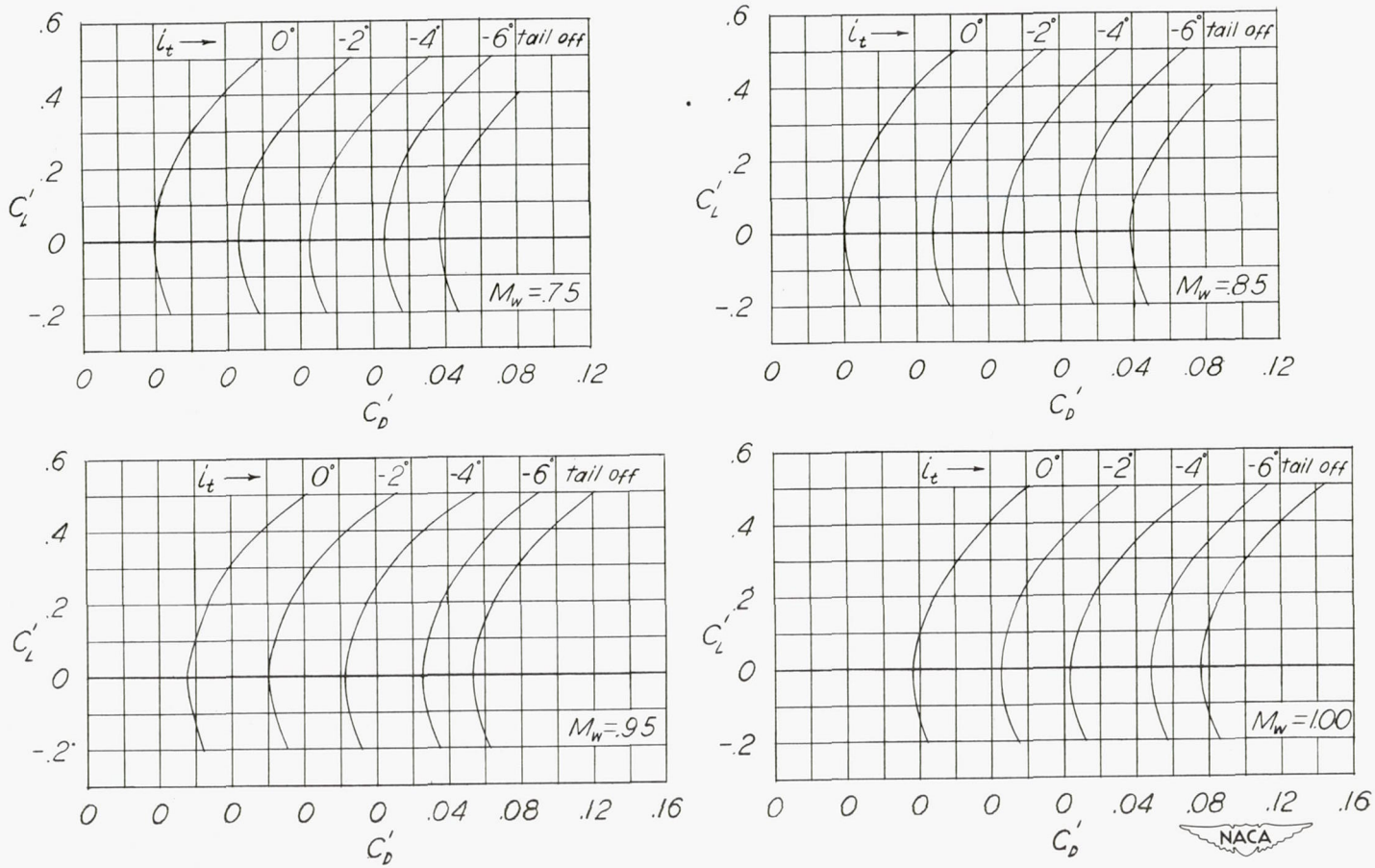

(a) $\Lambda = 60^\circ$.

Figure 12.- Variation of lift coefficient with drag coefficient for several tail incidences and wing sweepback angles at several Mach numbers for semispan model of Bell X-5 airplane. Results from reference 6 ($i_t = -2^\circ$) are also shown. (Coefficients based on 60° sweptback-wing dimensions.)

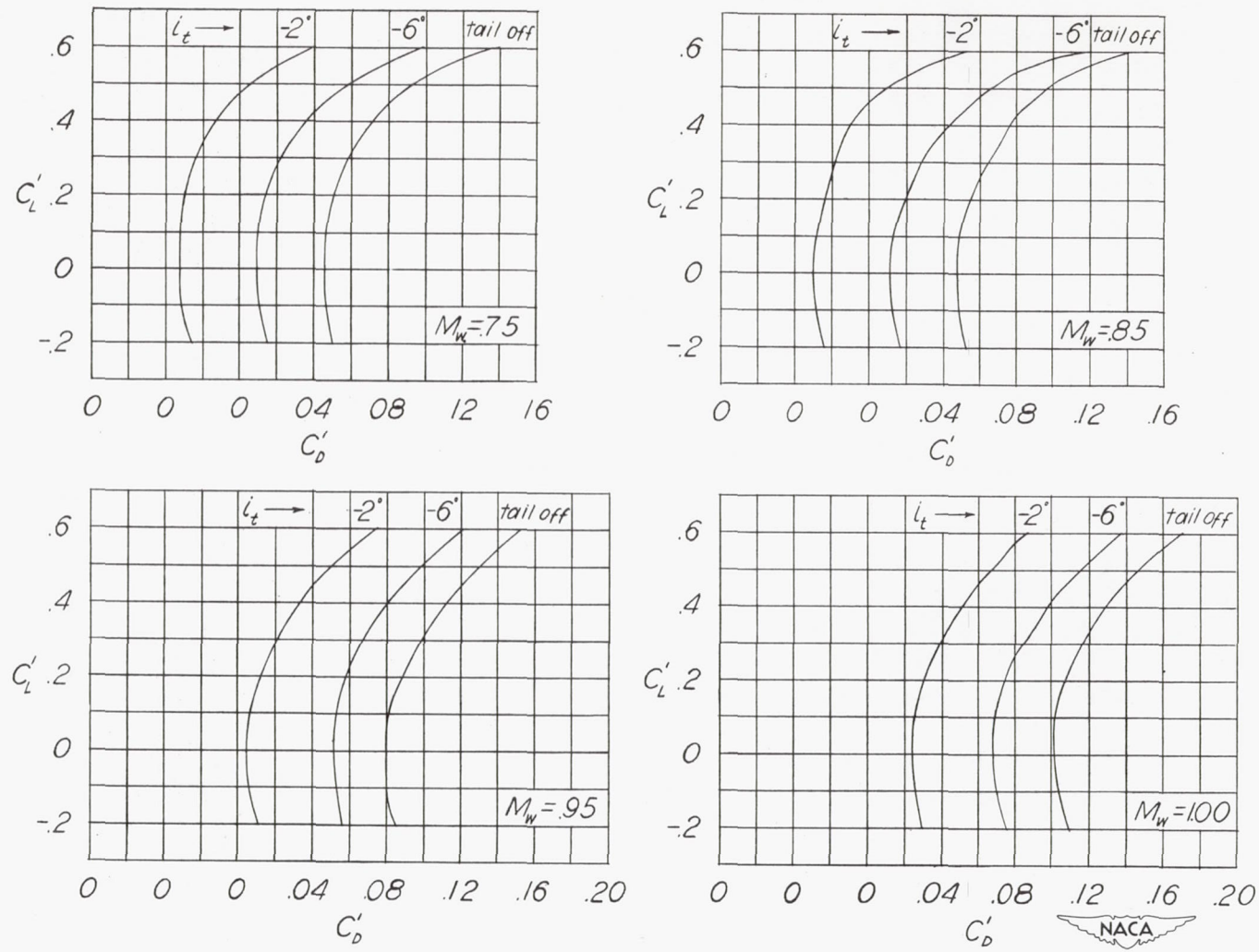

(b) $\Lambda = 40^\circ$.

Figure 12.- Continued.

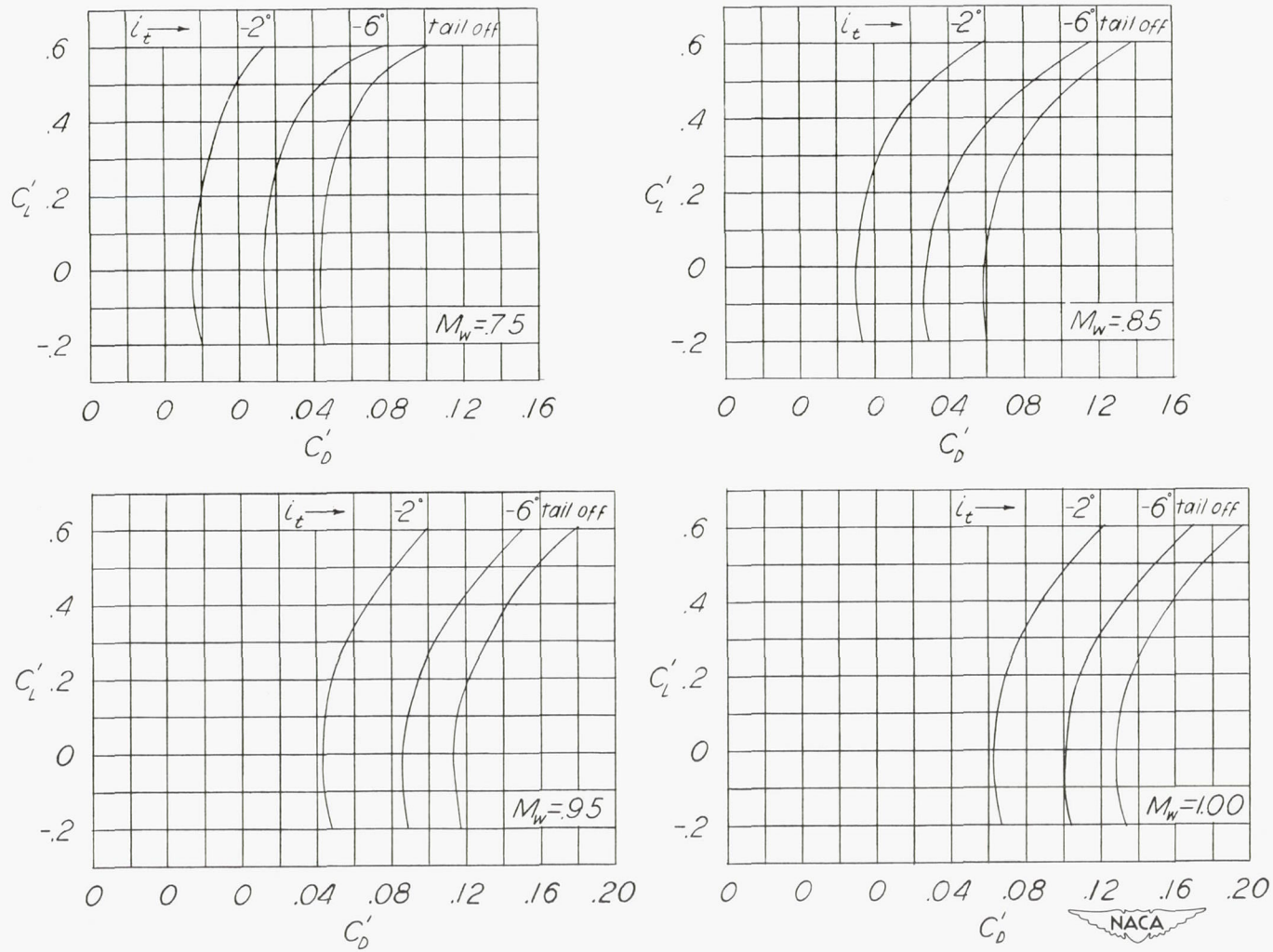

(c) $\Lambda = 20^{\circ}$.

Figure 12.- Concluded.

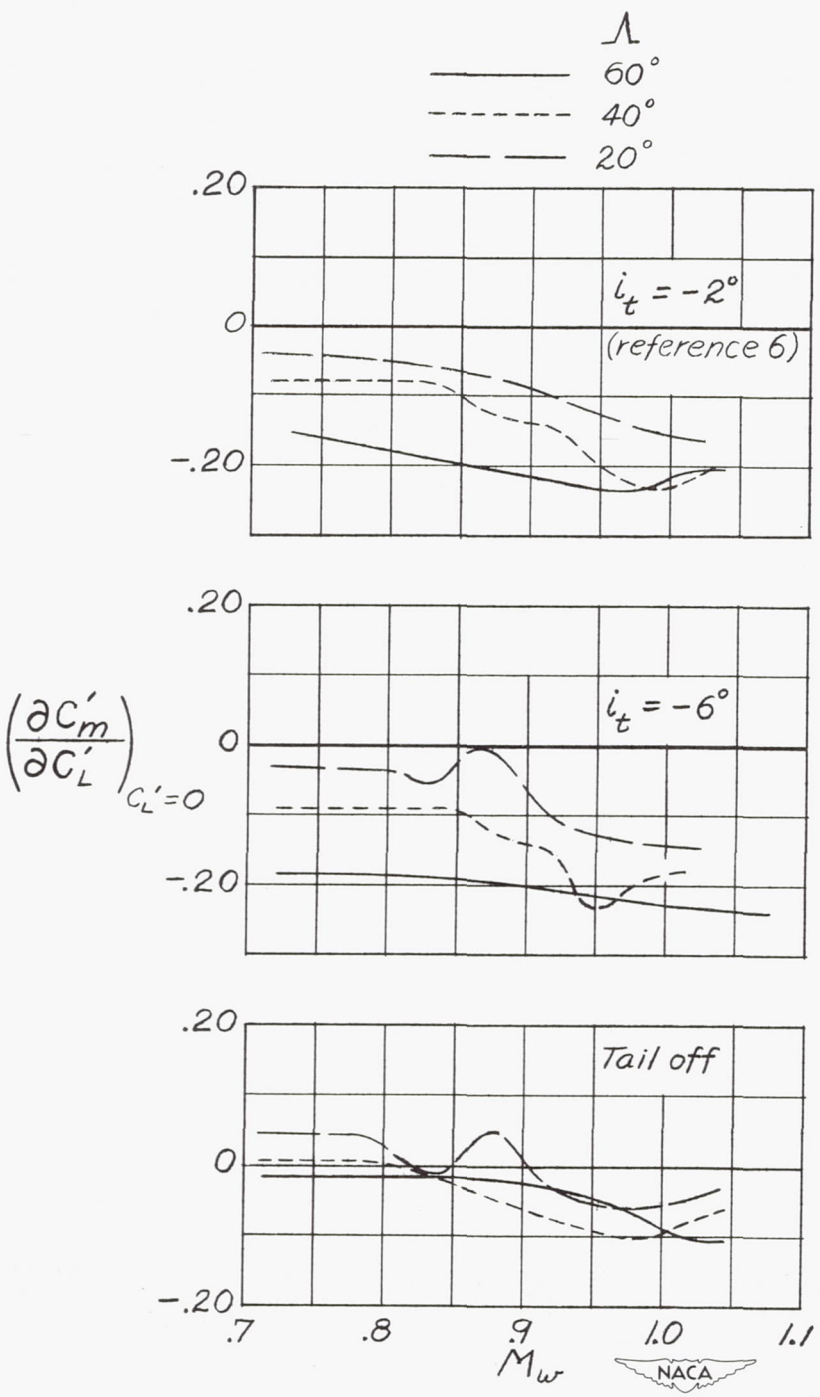

(a) $C_L' = 0$.

Figure 13.- Variation with Mach number of rate of change of pitching-moment coefficient with lift coefficient for several tail incidences and angles of sweepback at a lift coefficient of zero for semispan model of Bell X-5 airplane.

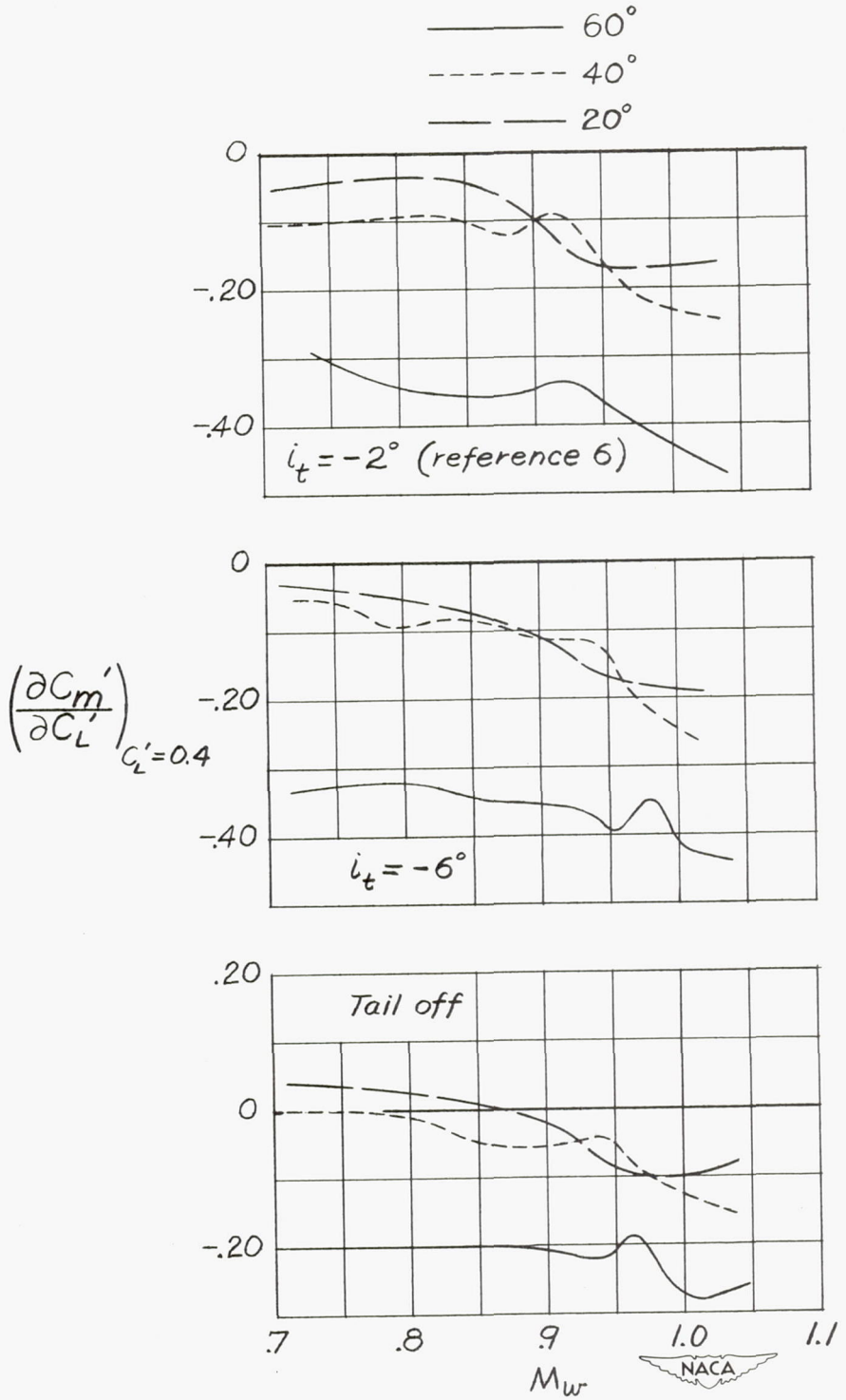

(b) $C_L' = 0.4$.

Figure 13.- Concluded.

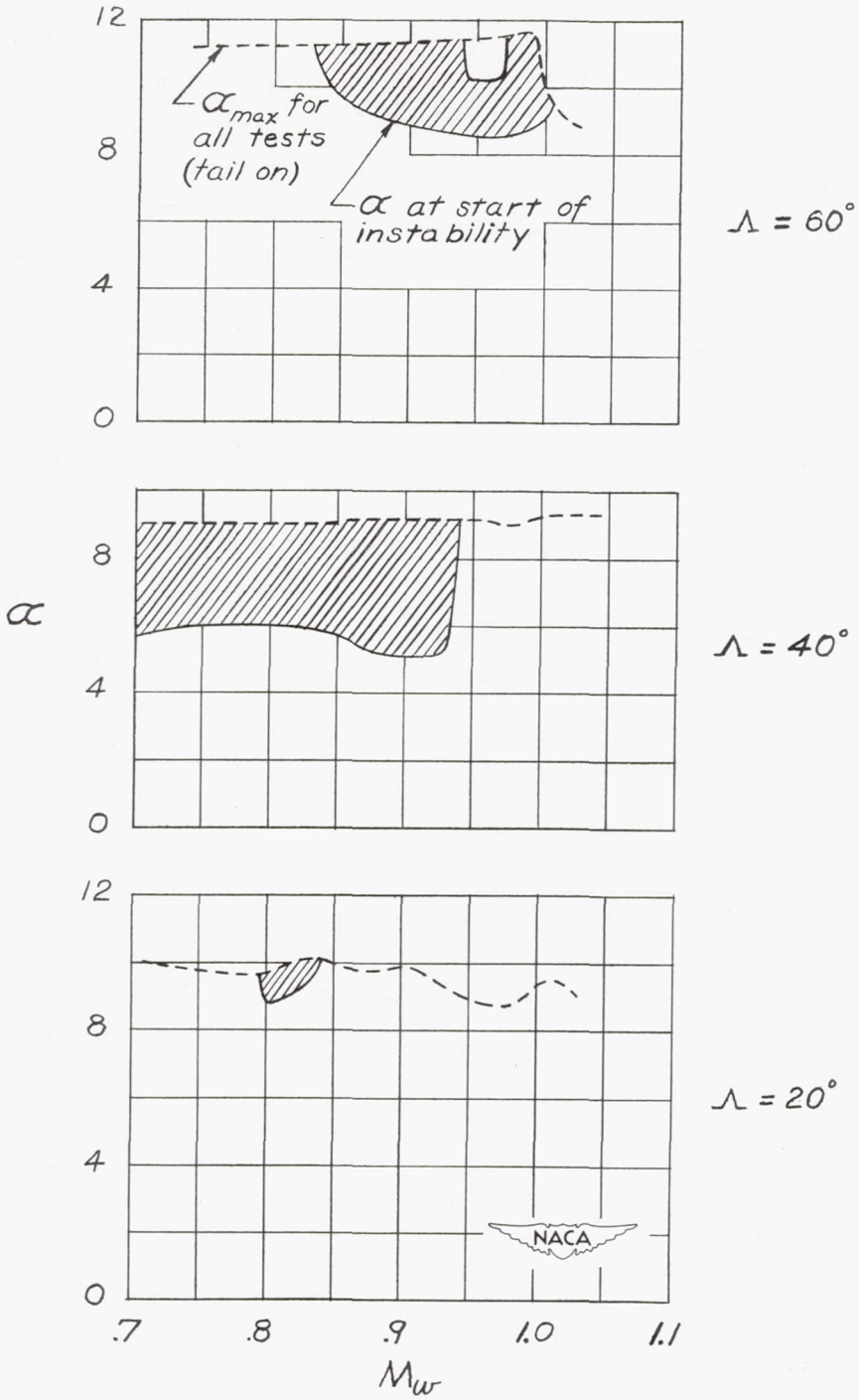

Figure 14.- Variation with Mach number of average angle of attack (solid line) for various tail incidences at which instability begins as determined by the departure of curve of C_m against α from a linear variation at high angles. Cross-hatched area indicates region of instability.

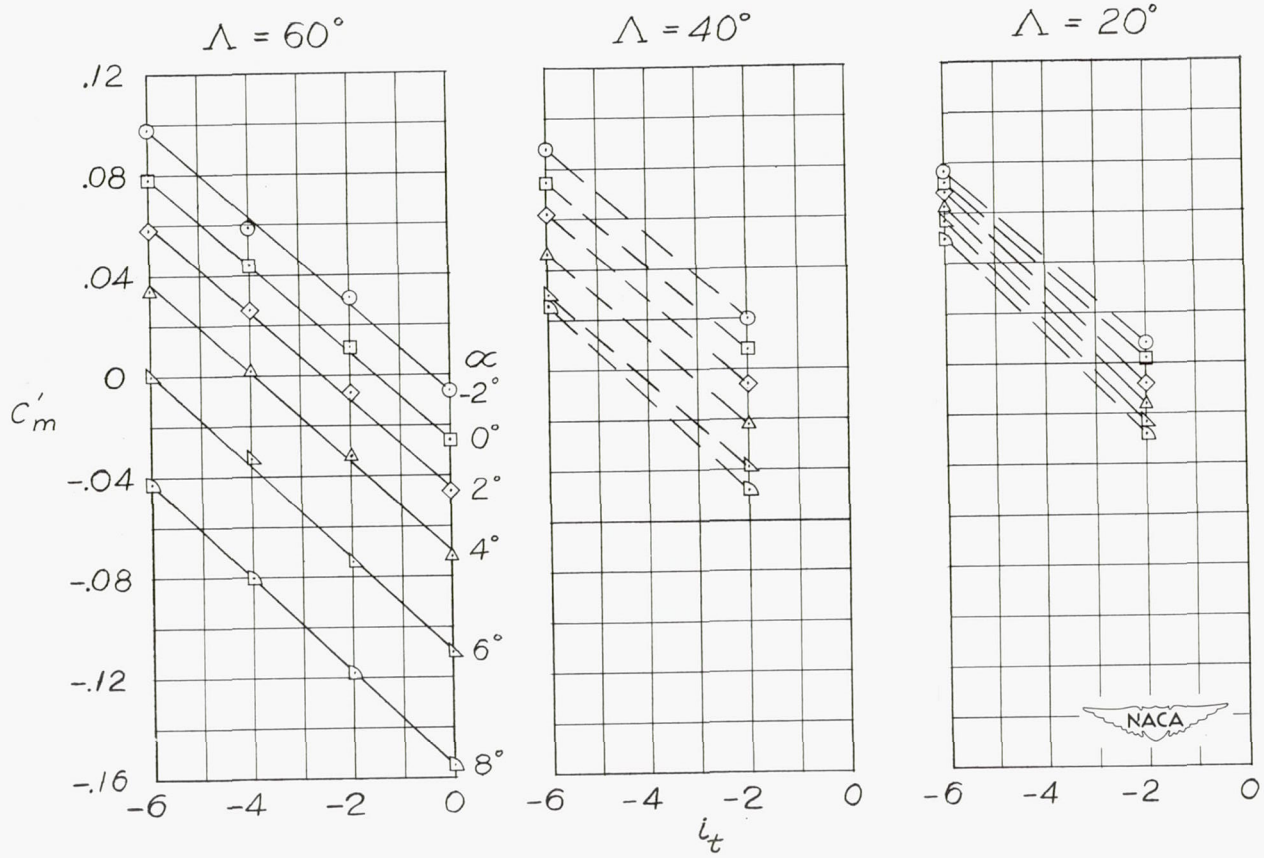

(a) $M_w = 0.75$.

Figure 15.- Variation of pitching-moment coefficient with tail incidence for several angles of attack and wing sweepback angles for semispan model of Bell X-5 airplane at several Mach numbers. Dashed lines indicate an approximate fairing due to limited number of test points. Data for $i_t = -2^\circ$ are taken from reference 6. (Coefficients based on 60° sweptback-wing dimensions.)

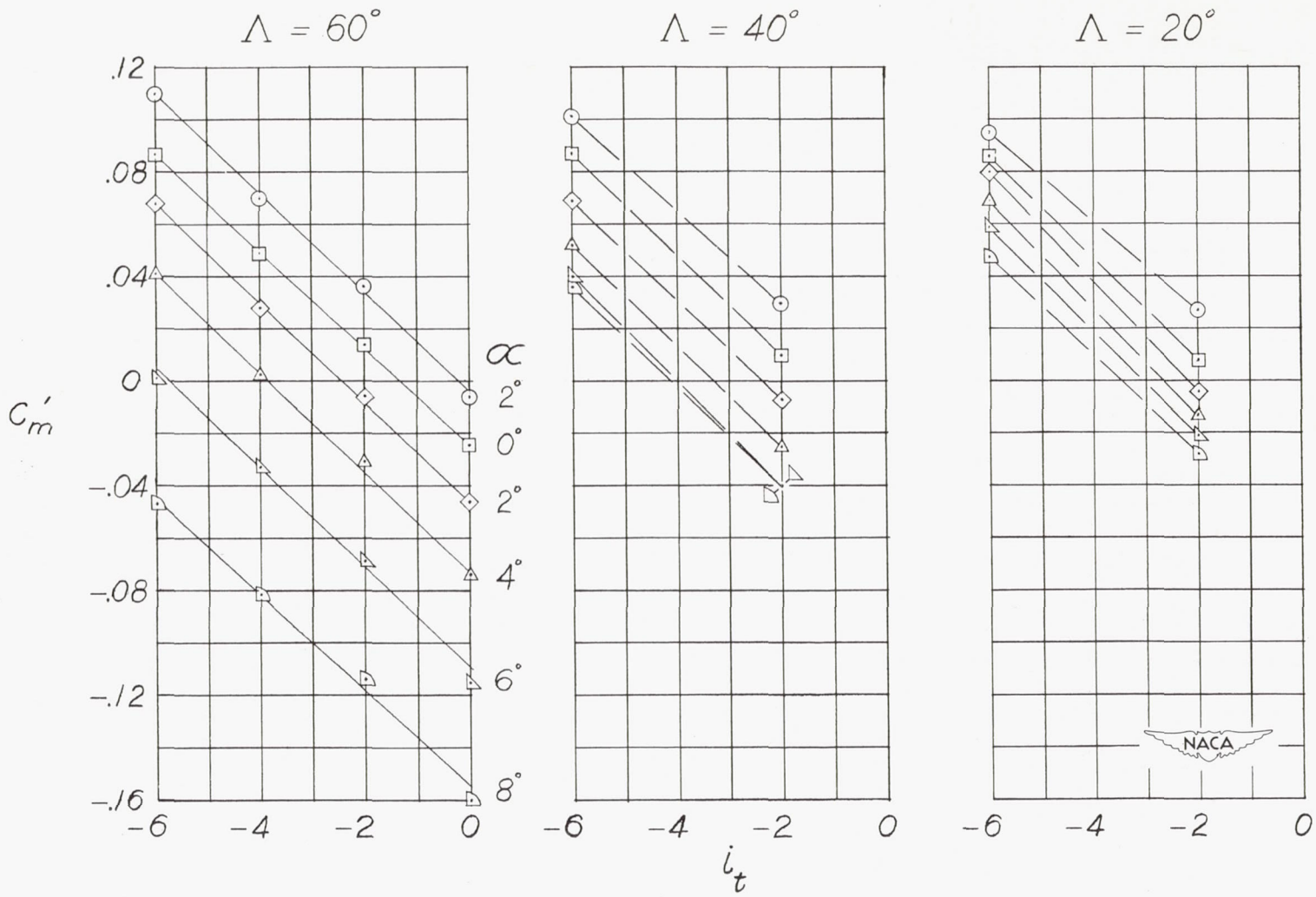

(b) $M_w = 0.85$.

Figure 15.- Continued.

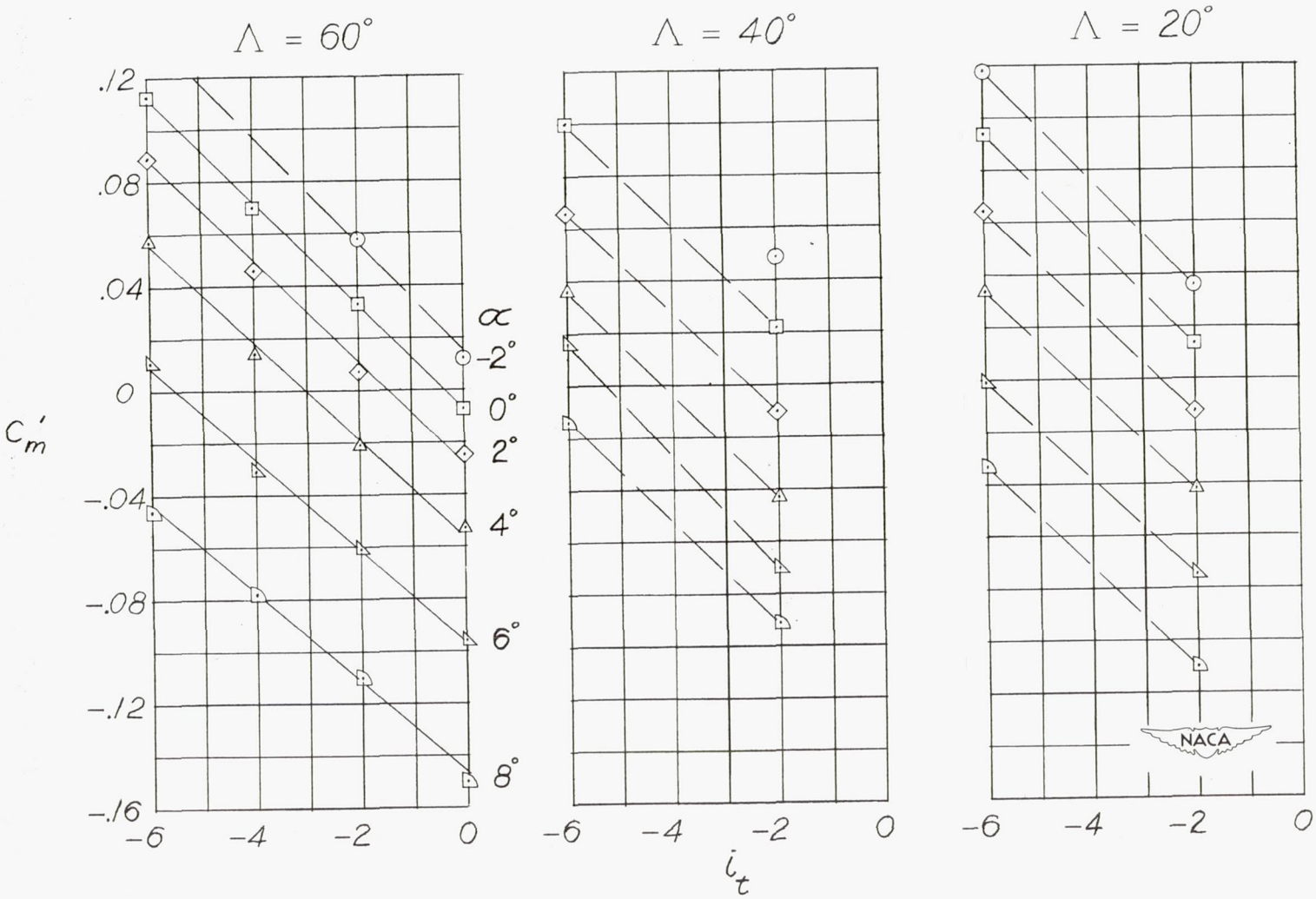

(c) $M_w = 0.95$.

Figure 15.- Continued.

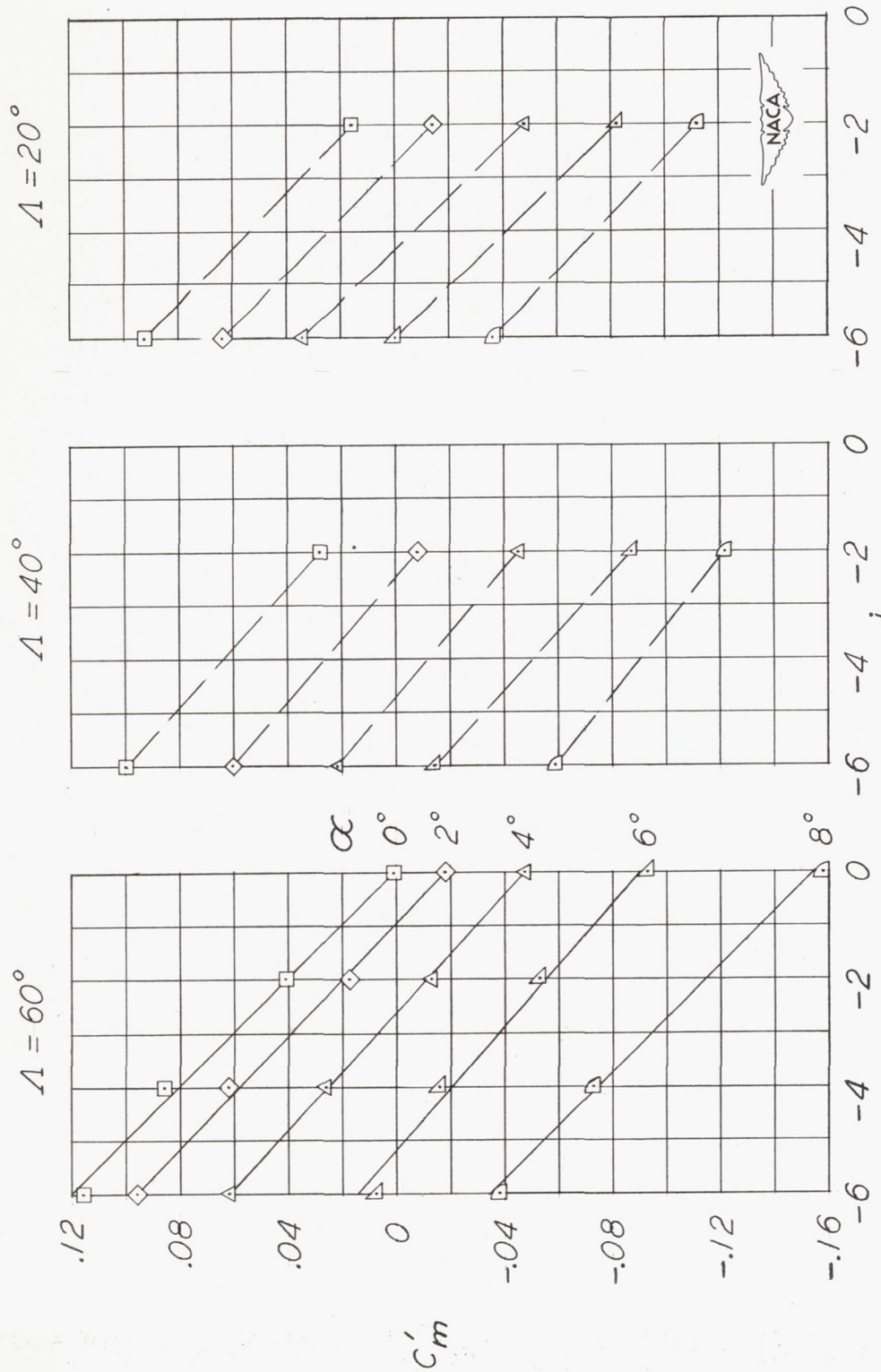

(d) M_w = 1.00.

Figure 15.- Concluded.

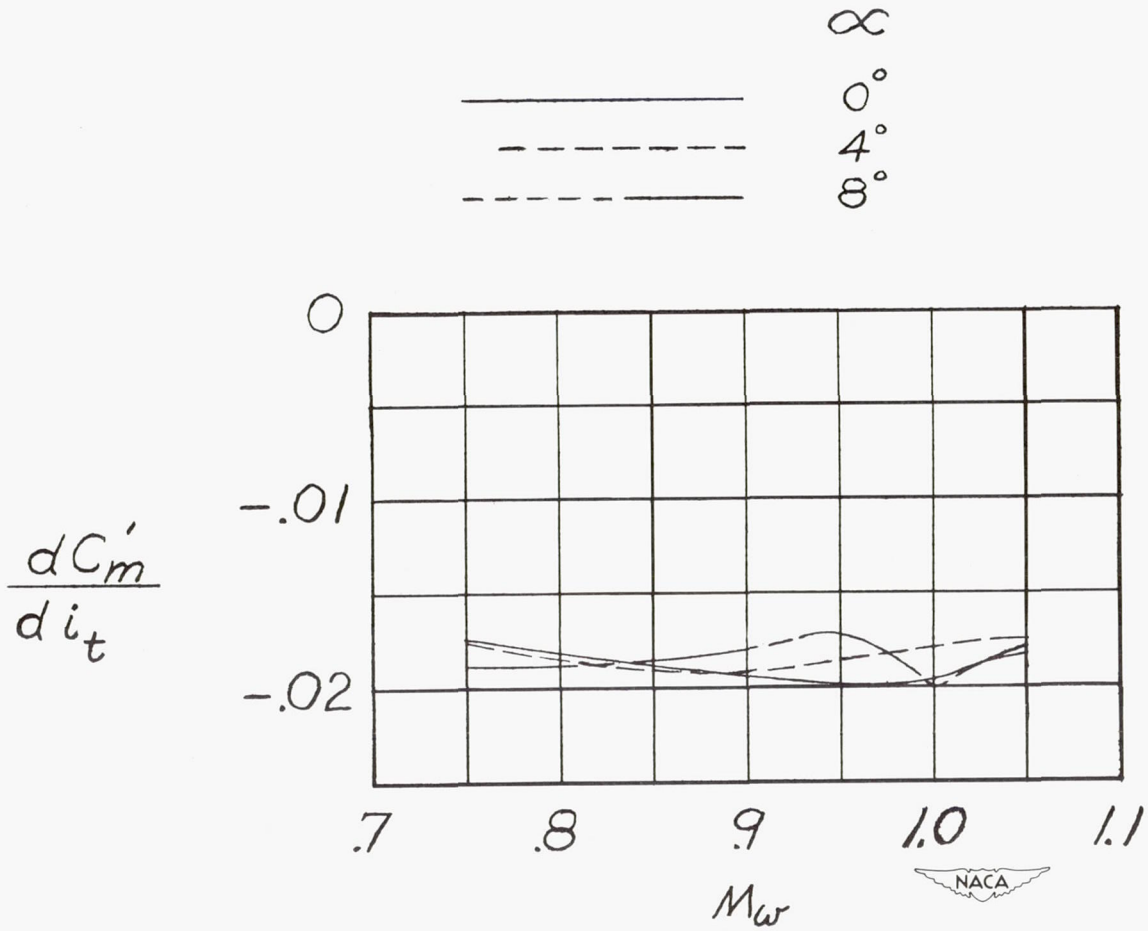

Figure 16.- Variation with Mach number of rate of change of pitching-moment coefficient with tail incidence at several angles of attack for semispan model of Bell X-5 airplane with 60° sweptback wing. (Coefficient based on 60° sweptback-wing dimensions.)

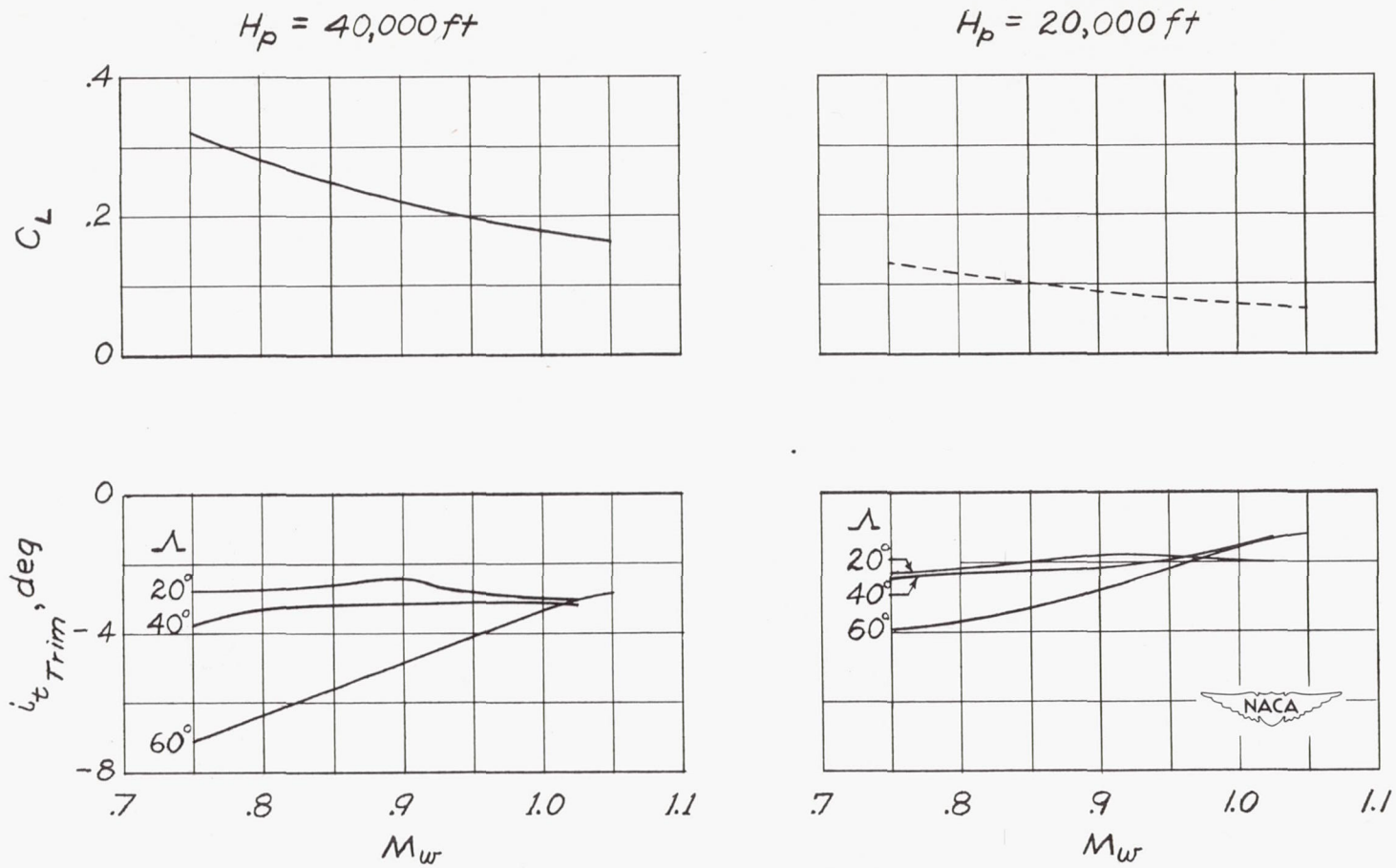

Figure 17.- Variation with Mach number of stabilizer angle required for trim in level flight at altitudes of 20,000 and 40,000 feet with wing loading of 50 and center of gravity located at 26 percent mean aerodynamic chord of 60° sweptback wing and at 35 percent mean aerodynamic chord of the 40° and 20° sweptback wings. Lift coefficient for level flight also shown.

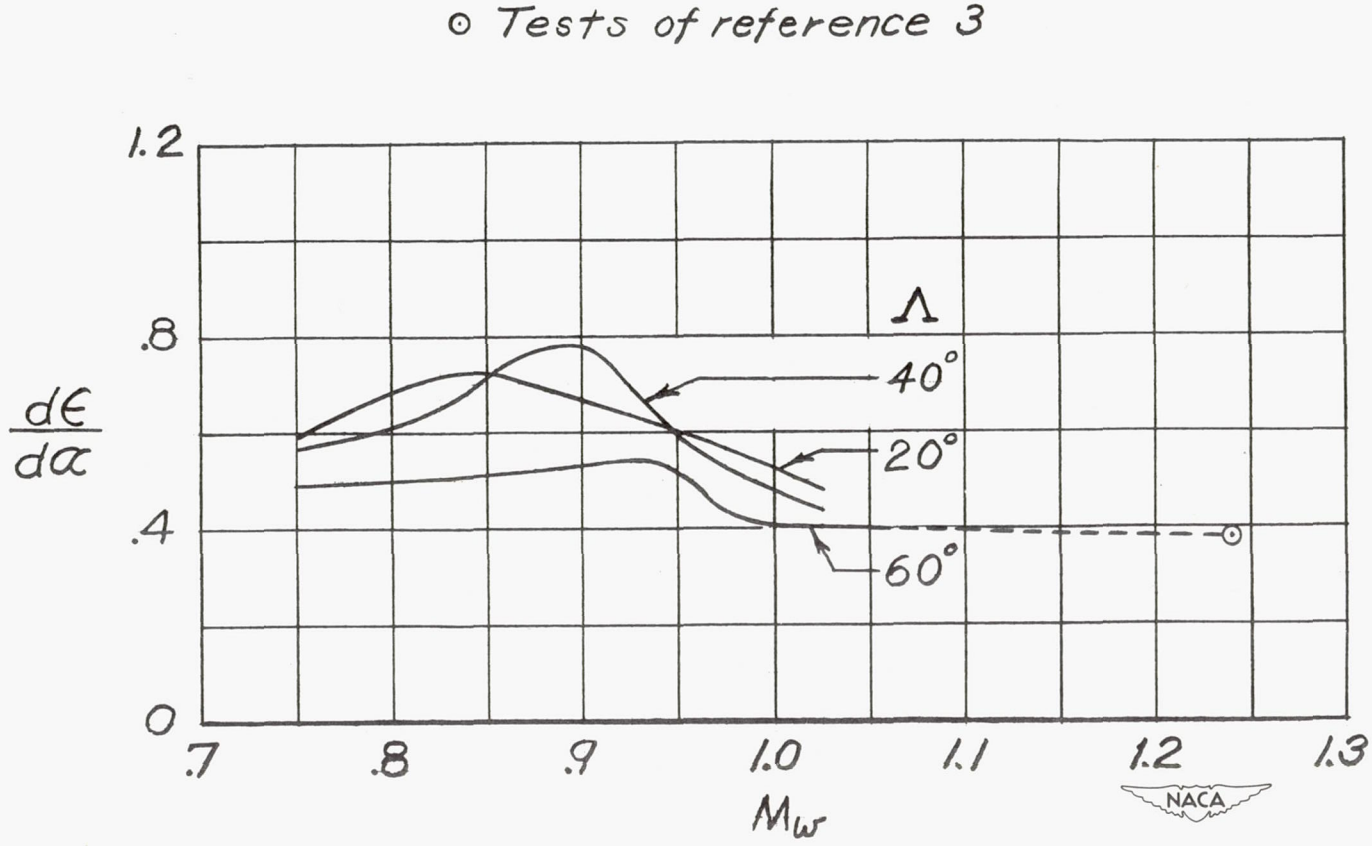

Figure 18.- Variation with Mach number of $d\epsilon/d\alpha$ for semispan model of Bell X-5 airplane with the wing swept back 60°, 40°, and 20°.